hLife ARTICLE

ppGpp is present in, and functions to regulate sleep of, *Drosophila*

Xihuimin Dai[1,2,#], Wei Yang[1,#], Xiaohui Zhang[3], Enxing Zhou[1], Renbo Mao[1], Ying Liu[3], Tao Wang[1], Wenxia Zhang[1], Xinxiang Zhang[4], Yi Rao[1,5,*]

*Correspondence: yrao@pku.edu.cn (Y.R.)
Received: September 3, 2023; Revised: October 11, 2023; Accepted: October 12, 2023
Doi:10.1016/j.hlife.2023.10.004

Citation: Dai X, Yang W, Zhang X, et al. ppGpp is present in, and functions to regulate sleep of, *Drosophila*. *hLife* 2023;1:98–114.

GRAPHICAL ABSTRACT

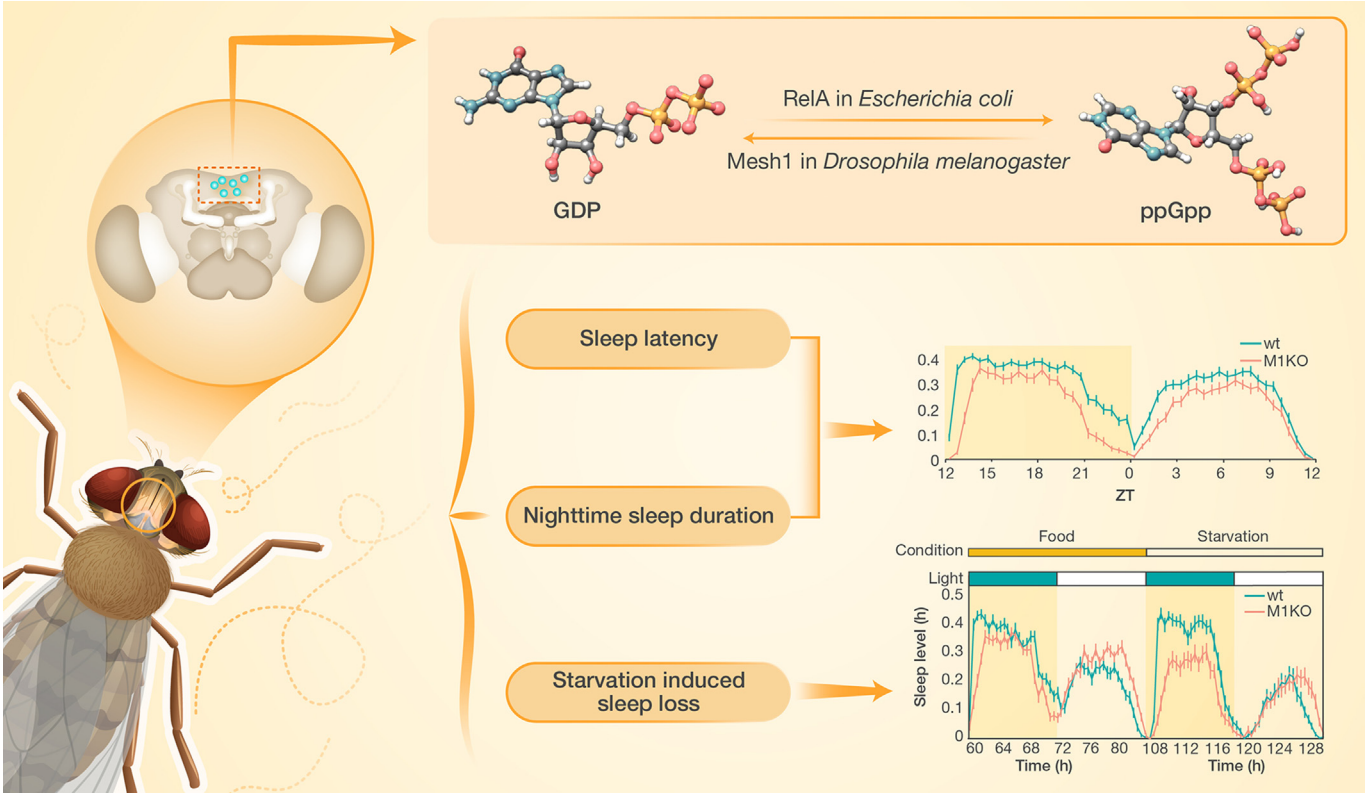

HIGHLIGHTS

- **Guanosine-5′-diphosphate, 3′-diphosphate (ppGpp) is present and hydrolyzed by mesh1 in *Drosophila.***
- **Nighttime sleep is decreased, and sleep latency is increased in flies with increased levels of ppGpp.**
- **Starvation-induced sleep loss (SISL) is exacerbated by increasing ppGpp levels in flies.**
- **Mesh1 expressed in Dilp2 neurons is essential for sleep and SISL regulation.**

ppGpp is present in, and functions to regulate sleep of, *Drosophila*

Xihuimin Dai[1,2,#], Wei Yang[1,#], Xiaohui Zhang[3], Enxing Zhou[1], Renbo Mao[1], Ying Liu[3], Tao Wang[1], Wenxia Zhang[1], Xinxiang Zhang[4], Yi Rao[1,5,*]

[1]Peking-Tsinghua Center for Life Sciences, PKU-IDG/McGovern Institute for Brain Research, Peking University School of Life Sciences, and Chinese Institute for Brain Research, Beijing, China
[2]Howard Hughes Medical Institute, Department of Biology, Brandeis University, Waltham, United States
[3]State Key Laboratory of Natural and Biomimetic Drugs, Peking University, Beijing, China
[4]College of Chemistry and Molecular Engineering, Peking University, Beijing, China
[5]Capital Medical University, Beijing, China
[#]These authors contributed equally to this work
*Correspondence: yrao@pku.edu.cn (Y.R.)
Received: September 3, 2023; Revised: October 11, 2023; Accepted: October 12, 2023
Doi:10.1016/j.hlife.2023.10.004

Citation: Dai X, Yang W, Zhang X, et al. ppGpp is present in, and functions to regulate sleep of, *Drosophila*. *hLife* 2023;1:98–114.

ABSTRACT

Sleep is essential for animals, and receives inputs from circadian, homeostasis, and environment, yet the mechanisms of sleep regulation remain elusive. Discovery of molecules in living systems and demonstration of their functional roles are pivotal in furthering our understanding of the molecular basis of biology. Here, we report that guanosine-5′-diphosphate, 3′-diphosphate (ppGpp) is present in *Drosophila*, and plays an important role in regulation of sleep and starvation-induced sleep loss (SISL). ppGpp is detected in germ-free *Drosophila* and hydrolyzed by an enzyme encoded by the *mesh1* gene in *Drosophila*. Nighttime sleep and SISL were defected in *mesh1* mutant flies, and rescued by expression of wildtype Mesh1, but not the enzymatically defective mutant Mesh1E66A. Ectopic expression of RelA, the *Escherichia coli* synthetase for ppGpp, phenocopied *mesh1* knockout mutants, whereas overexpression of Mesh1 resulted in the opposite phenotypes, supporting that ppGpp is both necessary and sufficient in sleep regulation. A chemo connectomic screen followed by genetic intersection experiments implicates the Dilp2 neurons in the *pars intercerebralis* (PI) brain region as the site of ppGpp function. Our results have thus validated the presence of ppGpp in *Drosophila* and revealed a physiological role of ppGpp in sleep regulation for the first time.

KEYWORDS sleep; Mesh1; *Drosophila*; ppGpp; starvation

INTRODUCTION

It was 50 years ago when guanosine-5′-diphosphate, 3′-diphosphate (guanosine tetraphosphate, ppGpp) and guanosine-5′-triphosphate, 3′-diphosphate (guanosine pentaphosphate, pppGpp) were implicated in gene regulation in *Escherichia coli* [1]. Collectively known as (p)ppGpp, they are key players in bacterial stringent response to amino acid starvation [2–9]. The level of ppGpp is regulated by the RelA/SpoT Homolog (RSH) family [10,11]. In bacteria, RelA is one of the RSHs [10], which contains both a ppGpp synthetase domain (SYNTH) and an inactive ppGpp hydrolase domain (HD) [11]. When amino acids are depleted, uncharged tRNAs accumulate [12] and activate the ribosome-associated RelA [13], which increases the production of ppGpp [14]. Another typical RSH in bacteria is the ppGpp hydrolase SpoT [15], containing a weak SYNTH [16] and an active HD [17]. Upon iron limitation [18], carbon starvation [19], or glucose phosphate stress [20], ppGpp was also increased [8].

ppGpp has also been detected in plants [21–27]. More than 30 members of the RSHs have been found in bacteria and plants [3,28].

(p)ppGpp has not been detected in animals until very recently. Early detection of ppGpp in the mouse turned out to be irreproducible [29–31]. Work in mammalian cell lines also failed to detect ppGpp before or after amino acid deprivation [32–42]. In *Drosophila*, metazoan SpoT homolog-1 (Mesh1), a member of the RSH family containing only the hydrolase domain for ppGpp has been found [43]. And during the submission of this work, ppGpp has just been reported to be detected in *Drosophila* and human cells and plays an important role in metabolism [44].

Drosophila has been served as a model for genetic studies of sleep for more than two decades [45,46]. Fly sleep is regulated by multiple genes functioning in several brain regions such as the fan-shape bodies (FSBs), the ellipsoid body (EB), the mushroom bodies (MB), and the *pars intercerebralis* (PI) [47,48].

Besides the internal control from circadian and homeostasis, sleep is also regulated by environmental factors such as food. Starvation has been found to induce sleep loss in both flies and mammals [49,50].

We have carried out a genetic screening for genes involved in sleep regulation [51,52] and here report that ppGpp is present in flies and regulates both daily sleep and starvation-induced sleep loss. *mesh1*, the gene encoding ppGpp hydrolase, is expressed in a specific population of neurons, and the effects of RelA, the bacterial ppGpp synthetase, and Mesh1 overexpression could be detected when they were expressed in neurons, but not in non-neuronal cells. Further dissection narrowed down the functional significance of *mesh1*-expressing neurons in the PI. Thus, after more than 50 years of its discovery, we have confirmed the presence of ppGpp in animals and first found that it functions in sleep regulation in specific neurons.

RESULTS

ppGpp is Present and Regulated by *mesh1* in *Drosophila*

We screened through 1765 P-element insertion lines of *Drosophila* [53] for mutations affecting sleep latency (Figure 1A), and found that an insertion in the *mesh1* gene (*mesh1*-ins) (Figure 1C) resulted in significantly longer sleep latency (Figure 1A and 1D) and less total sleep duration (Figure 1B).

mesh1 encodes an RSH family member in animals, and Mesh1 protein is predicted to have hydrolase activity, converting ppGpp to GDP [43] (Figure 1E). However, ppGpp has not been detected in animals until very recently [44], and the function of Mesh1 remains largely unknown.

Through expression, purification, and an *in vitro* hydrolysis assay of *Drosophila* Mesh1 protein in *E. coli*, we found that ppGpp was indeed degraded by Mesh1 *in vitro* (Figure S1A). To test the existence of endogenous ppGpp in *Drosophila*, extracts from more than 2000 flies were made. ppGpp was detected by ultra-performance liquid chromatography and mass spectrometry (UPLC-MS) in wild type (wt) flies (Figure 2A and 2B). We generated a knockout (KO) line of *mesh1* (*M1KO*) using CRISPR-Cas9 to replace most of its coding sequence following the start codon with 2A-attP (Figure 1C) and found that more ppGpp was present in *M1KO* flies than the wt flies (Figure 2C), consistent with the fact that *Drosophila mesh1* encodes only a hydrolase domain (Figure S1B). Thus, the ppGpp detected by us was regulated by the *Drosophila mesh1* gene.

To tell whether the detected ppGpp was synthesized by the flies or from bacteria attached to the flies, we generated germ-free lines of wt and *M1KO* for analysis. We confirmed that the flies were indeed germ-free flies with both bacterial culture (Figure S1C) and 16S ribosomal DNA gene polymerase chain reaction (16S rDNA PCR) (Figure S1D). Because ppGpp is known to be involved in starvation response in bacteria [8,54], and *mesh1* mutant flies have been reported to have impaired starvation resistance [43], we tested ppGpp in fed and starved flies. ppGpp was detected in both fed and starved germ-free flies, and levels in *M1KO* were significantly higher in both conditions (Figure 2D-2G), suggesting that flies can indeed synthesize ppGpp.

Taken together, our results indicate that ppGpp is present in *Drosophila* and is regulated by *mesh1* gene.

Decreased Sleep at Early Night and Late Night in *mesh1* Mutants

Because we identified mesh1 mutant through a sleep screen, we then looked at the sleep profiles of *M1KO* mutant flies. *M1KO* flies sleep significantly less than wt flies and showed shifted activity peaks (Figure 3A). In the paradigm of 12 h of light and 12 h of darkness (Light:Darkness, LD), *M1KO* flies showed significantly decreased nighttime sleep (Figure 3B), decreased total sleep (Figure 3D) and increased sleep latency at night (Figure 3E), but no significant change in daytime sleep level (Figure 3C) or daytime sleep latency (Figure 3F) was detected. Sleep bout number and length were not significantly different between wt and *M1KO* flies (Figure S2).

We assessed awakening according to a procedure reported recently [55]. Awakening number at the beginning of nighttime sleep (early night) (Figure 3G) and awakening number near the end of nighttime sleep (late night) (Figure 3H) were significantly increased in *M1KO* mutants.

Taken together, these results showed that it takes longer for *M1KO* flies to fall asleep at early night, and they wake up earlier in the late night, indicating a role of *mesh1* in regulating sleep latency at early night and awakening at late night.

The Enzymatic Activity of *mesh1* is Essential to Sleep

Next, we asked whether the enzymatic activity of *mesh1*, which hydrolyzes ppGpp, is important to sleep. A previous *in vitro* study has shown that an E66A mutation in Mesh1 protein significantly disrupts the ppGpp hydrolase activity [43]. Consistent with the previous study, we found that when expressed in bacteria, Mesh1E66A could not hydrolyze ppGpp (Figure S1A).

To enable manipulation of *mesh1*-expressing cells, we generated a KO-Gal4 line of *mesh1* (*M1KOGal4*) by replacing its coding sequence (CDS) after the start codon with an in-frame fusion of the 2A peptide and the yeast transcription factor Gal4 (Figure 4A). We then expressed wildtype Mesh1 and Mesh1E66A respectively in *mesh1*-expressing cells of the mutant flies driven by *M1KOGal4*. We found that compared with *M1KO* mutant flies, the level of ppGpp in flies was rescued to control group level by expression of wildtype Mesh1, but could not be rescued by expression of Mesh1E66A (Figure S1E). These results indicate that wt Mesh1 protein could, but Mesh1 E66A mutant protein could not, hydrolyze ppGpp either *in vitro* or *in vivo*.

We then looked at whether wildtype Mesh1 and Mesh1E66A could rescue the sleep phenotypes of longer sleep latency (Figure 4B), increased awakening number at early night (Figure 4C) and late night (Figure 4D). We found that expression of wildtype Mesh1 driven by *M1KOGal4* rescued all these phenotypes (Figure 4B–4D). By contrast, expression of Mesh1E66A could not rescue the sleep phenotypes in *M1KOGal4*/*M1KO* flies (Figure 4B–4D).

Taken together, the *in vitro* results from bacterially expressed Mesh1 and Mesh1E66A proteins and the *in vivo* results from genetic rescue experiments in flies strongly support that Mesh1 functions through ppGpp to regulate sleep.

mesh1 is Expressed in the Nervous System of *Drosophila*

To examine the expression pattern of Mesh1, we utilized the Gal4-UAS system to express different effectors behind UAS in

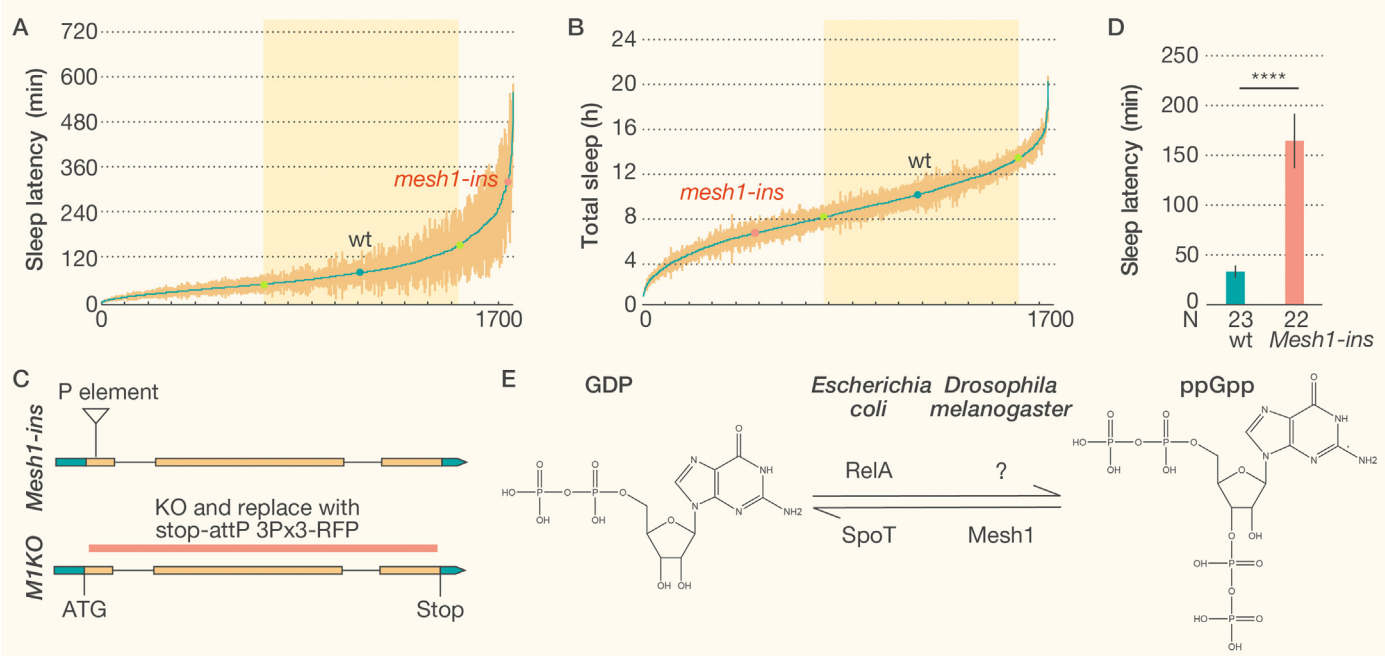

Figure 1. Results of a sleep latency screen

Sleep latency (A) and total sleep duration (B) results of a screen of 1765 P-element insertion lines. *mesh1-ins* flies had significant longer sleep latency (A) and less total sleep (B) than wild type (wt) flies. *y* axis is sleep latency in minutes and total sleep in hours respectively, and *x* axis is screened P element insertion lines. Shadows indicate the standard error of the mean (SEM) from multiple flies of each line, and green dots and yellow rectangles show the range of 3-fold of standard deviation from the value of wt. (C) Schematic representations of *mesh1*-ins and knockout (KO) line of *mesh1* (*M1KO*) genotypes. In *mesh1-ins*, the P-element was inserted into the coding sequence (CDS) of the first exon. In *M1KO*, the entire CDS except the start codon was replaced with stop-2A-attP and 3Px3-RFP. (D) Statistical analysis. Sleep latency was significantly longer in *mesh1*-ins flies (Student's *t*-test, ****$P < 0.0001$). Error bars represent SEM. The number of flies used in the experiment was denoted under each bar. (E) A diagram of guanosine-5′-diphosphate, 3′-diphosphate (ppGpp) metabolism. In *E. coli*, GDP is converted to ppGpp by its synthetase RelA, whereas ppGpp is converted to GDP by the hydrolase SpoT. In *D. melanogaster*, only the hydrolase Mesh1 has been discovered but the synthetase is unknown.

Mesh1-expressing cells labeled by *M1KOGal4*. We crossed *M1KOGal4* with each of the following four UAS lines: *UAS-mCD8-GFP* for cell membrane labeling [56], *UAS-redStinger* for nuclei labeling [57], *UAS-denmark* for dendrites labeling [58] and *UAS-syt::eGFP* for axon terminals labeling [59].

We found that Mesh1 is expressed in neurons in the central brain and the ventral nerve cord (VNC) (Figure 5A and 5B). In the central brain, *mesh1*-expressing neurons were detected in the PI and the suboesophageal ganglia (SOG) (Figure 5E). The *mesh1*-expressing neurons in the PI (Figure 5A) with their axonal terminals in the SOG (Figure 5D and 5E) were reminiscent of the insulin-producing cells (IPC) in the PI which were shown previously to regulate sleep [60].

Neuronal ppGpp Regulates Sleep

Other than the role in ppGpp hydrolysis, Mesh1 has also been found to serve other functions in mammalian cells, such as nicotinamide adenine dinucleotide phosphate (NADPH) phosphatase [61]. To further investigate the role of ppGpp in sleep regulation, we ectopically expressed the *E. coli RelA* gene, which encodes a synthetase for ppGpp [15] in different sets of neurons.

Firstly, we confirmed that the RelA from *E. coli* used by us indeed can increase ppGpp level *in vitro* (Figure S1A). We then expressed RelA in neurons labeled by different drivers using Gal4-UAS system to specifically increase the ppGpp level in them. Because RelA and Mesh1 serve opposite functions in ppGpp metabolism, RelA expression would phenocopy *mesh1* mutant flies if mesh1 functions through ppGpp to regulate sleep. We found that when RelA was expressed in all the cells driven by *tub-Gal4* [62], or in all the neurons driven by *elav-Gal4* [63], sleep latency (Figure 6A) and awakening numbers at early night (Figure 6B) were significantly increased, phenocopying *M1KO* flies (Figure 6A and 6B). By contrast, *UAS-RelA* driven by *repo-Gal4* for expression in glial cells [64] did not affect sleep (Figure 6A and 6B). These results indicate that ppGpp functions in neurons, but not in glial cells, to regulate sleep.

Furthermore, when RelA was specifically expressed in *mesh1*-expressing cells labeled by *M1KOGal4*, both sleep latency (Figure 6A) and awakening numbers (Figure 6B) were significantly increased, indicating that ppGpp level in *mesh1* positive neurons is sufficient to regulate sleep.

To test the effect of decreasing ppGpp level in different fly cells, we overexpressed *UAS-mesh1* in these drivers. Similar with RelA ectopic expression, *UAS-mesh1* overexpression driven by *tub-Gal4* in all cells or by *elav-Gal4* in neurons significantly decreased sleep latency (Figure 7A) and awakening numbers (Figure 7B). By contrast, *UAS-mesh1* overexpression driven by *repo-Gal4* in glial cells did not affect sleep latency or awakening numbers (Figure 7A–7C).

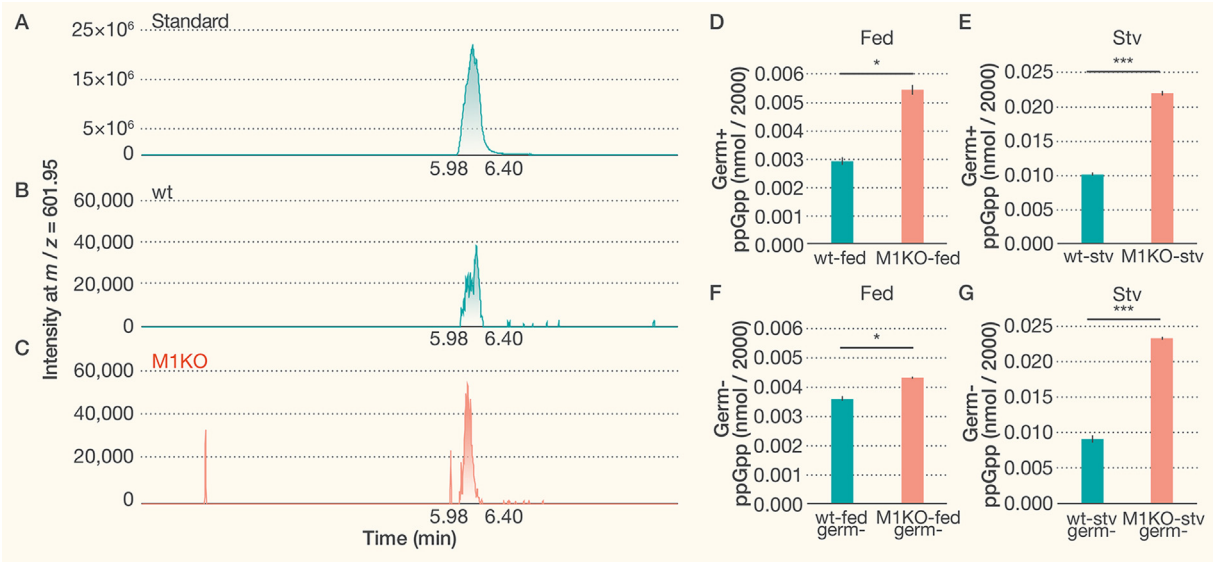

Figure 2. Identification and quantitative analysis of guanosine-5′-diphosphate, 3′-diphosphate (ppGpp) in *Drosophila*
UPLC-MS profiles of standard ppGpp (A), extracts of wt flies (B), and extracts of *M1KO* flies (C). ppGpp is detected in wt flies and increased in *M1KO* flies. *x* axis is time (minutes), and *y* axis is intensity of MS signal at *m/z* = 601.95, which corresponds to standard ppGpp. Statistical analyses of ppGpp level under fed (D, F) and starved (E, G) conditions in normal flies (D, E) and germ-free flies (F, G). For each group, ~2000 male flies were sacrificed for UPLC-MS measurements. In all conditions, ppGpp level was significantly increased in *M1KO* flies compared with wt flies. Student's *t*-test was used, $*P < 0.05$, $***P < 0.001$. Error bars represent SEM. Flies in the starvation group are starved for 24 h.

Taken together, data from increasing or decreasing the ppGpp level by expressing RelA or Mesh1 with different drivers indicate that ppGpp functions in neurons but not in glia to regulate sleep.

ppGpp Functions in Dilp2 Neurons to Regulate Sleep

Our results have shown that ppGpp functions in neurons to regulate sleep (Figures 6A and B, 7A and 7B). Next, to find where does ppGpp function to regulate sleep in flies, we made use of a Gal4 library of the chemo connectome (CCT) previously generated by us, which include all the known neurotransmitters, modulators, neuropeptides and their receptors [65]. We carried out a CCT screen by crossing each Gal4 line with *UAS-RelA*. We found that RelA expression driven by Gal4 lines of Trh, Capa-R, CCHa2-R, LkR, OA2, and CG13229 robustly affected sleep latency (Figure S3A). It was noted that all of these lines drove expression in the PI region (Figure S3B-S3G), which suggests a functional significance of *mesh1* expression in the PI region (Figure 5).

To further dissect the PI neurons for functional involvement in ppGpp regulation of sleep, we tested Gal4 lines known to drive expression in PI neurons: *Dh44-Gal4* [66,67], *Dilp2-Gal4* [60,68,69] and *R19G10-Gal4* [70,71]. To confirm whether *mesh1* is expressed in the PI neurons labeled by these drivers, we generated a Flp line of *mesh1* (*M1KIflp*, Figure S4A), so that flippase will be expressed in *mesh1* cells and cut out the stop cassette flanked by FRT in *UAS-FRT-stop-FRT-mCD8-GFP*. In this way, GFP is expressed in cells that are labeled by both the PI driver and *mesh1*. We found that mesh1 is indeed expressed in the PI neurons labeled by *Dh44-Gal4*, *Dilp2-Gal4*, and *R19G10-Gal4* (Figure S4B-S4D). Also, co-expression of Dilp2 and Mesh1 was found by Dilp2 immunostaining of *M1KOGal4>UAS-mCD8-GFP* brains (Figure S4E).

We then investigated the function of ppGpp in these PI neurons by crossing the drivers with *UAS-RelA* to increase ppGpp level in the neurons. Sleep latency (Figure 6C) and awakening numbers (Figure 6D) were significantly increased by RelA expression in neurons labeled by *R19G10-Gal4* and *Dilp2-Gal4*. However, RelA expression in Dh44 neurons did not affect sleep (Figure 6C and 6D).

Each of these PI drivers was crossed with *UAS-Mesh1* to decrease ppGpp level in the neurons. Consistent with previous results, sleep latency (Figure 7D) and awakening numbers (Figure 7E) were decreased by Mesh1 expression in neurons labeled by *R19G10-Gal4* and *Dilp2-Gal4*, but not in Dh44 neurons (Figure 7D–7F).

Taken together, experiments with RelA ectopic expression and Mesh1 overexpression have provided consistent results indicating that ppGpp functions in Dilp2-positive and Dh44-negative PI neurons to regulate sleep.

ppGpp in Dilp2 Neurons Promotes Starvation-induced Sleep Loss

Sleep regulation gets input from many other activities, for example, starvation has been found to induce sleep loss in both humans [72] and flies [50]. Insulin signaling through Dilp2 plays a critical role in the interaction between diet and sleep homeostasis [73]. Previous studies have suggested that ppGpp in bacteria and Mesh1 in flies are important to starvation response [8,43,54]. Given the role of ppGpp in Dilp2 neurons in sleep regulation, we next investigated whether ppGpp regulates SISL.

Baseline sleep in fed flies was recorded before flies were starved for 24 h [69]. Sleep during starvation was compared to that before starvation (Figure 8A). Nighttime SISL in *M1KO* flies was significantly more than that in wt flies, whereas daytime

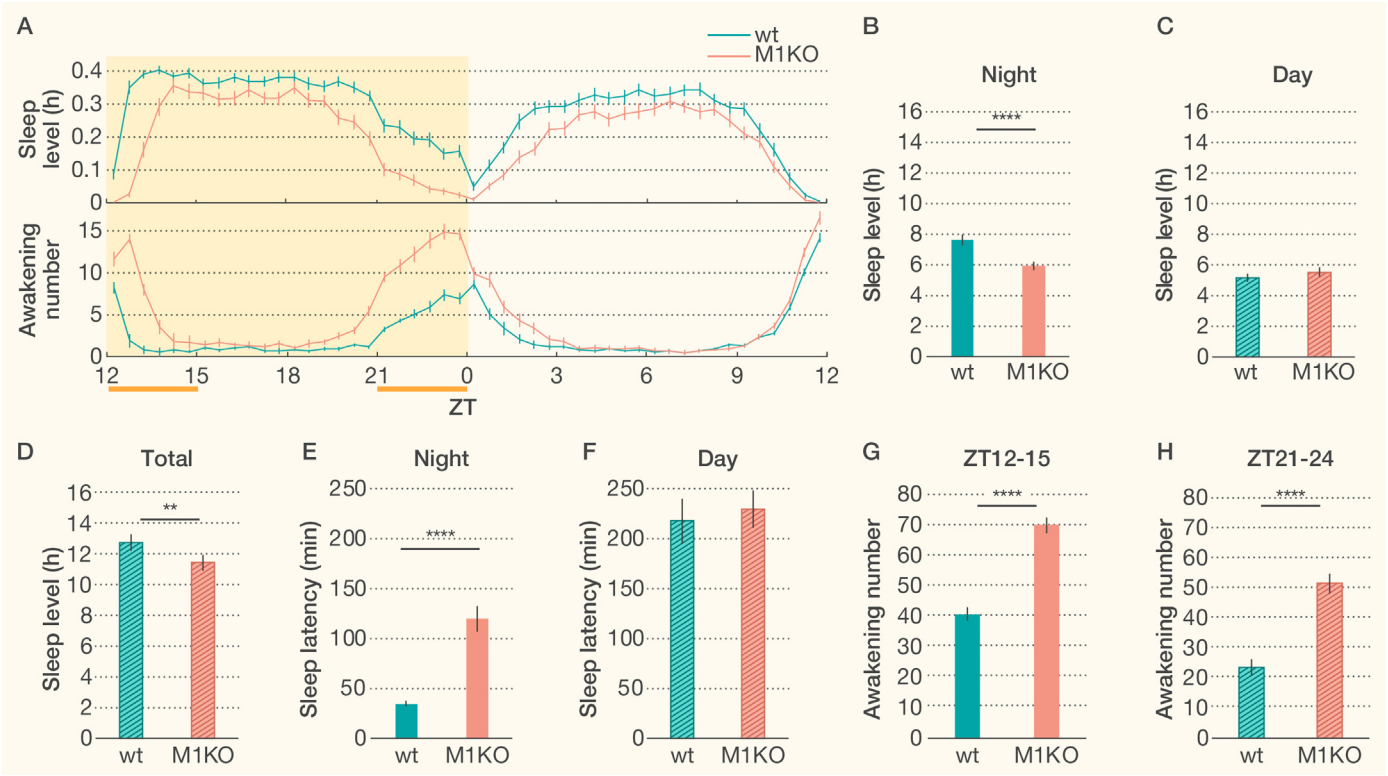

Figure 3. Sleep phenotypes of *M1KO* mutant flies
(A) Profiles of sleep (top) and awakening (bottom) in *M1KO* Flies, plotted in 30mins bins. Shaded background indicates the dark phase (ZT12-24); white background indicates the light phase (ZT0-12). Early night (ZT12–15) and late night (ZT21–24) were denoted with orange bars. Statistical analyses of sleep duration during nighttime (B), daytime (C) and in total (D). Nighttime and total sleep were significantly reduced in *M1KO* flies. Statistical analyses of sleep latency of nighttime (E) and daytime (F). Nighttime sleep latency was significantly increased in *M1KO* flies. Statistical analyses of summed awakening numbers at early night (G) and late night (H). Awakening numbers of both early night and late night were significantly increased in *M1KO* flies. Student's *t*-test, $^{**}P < 0.01$, $^{****}P < 0.0001$. Error bars represent SEM. 48 flies were used for each group. The experiments have been repeated at least three times with biological replicates.

SISL was similar between the wt and *M1KO* flies (Figure 8A and B).

We next investigated whether the enzymatic activity of Mesh1 is also important for SISL. The *M1KOGal4* mutants were similar to *M1KO* flies in having exacerbated SISL (Figures 8C and S5A-S5C). *UAS-mesh1* (Figures 8C and S5D) but not *UAS-mesh1E66A* (Figures 8C and S5E) could rescue the phenotype of SISL in *mesh1* knockout flies, indicating that the ppGpp hydrolyzing activity is required for Mesh1 involvement in SISL.

Ectopic expression of the bacterial ppGpp synthetase RelA in Mesh1-expressing cells caused an exacerbated SISL (Figure 8D), phenocopying *M1KO* flies. Oppositely, expression of Mesh1 in Mesh1-expressing cells resulted in an alleviated SISL (Figure 9A). Taken together, these results indicate that ppGpp level, rather than any other unexpected activities of RelA or Mesh1 were involved in the SISL phenotypes.

We then asked does ppGpp functions in the same set of cells to regulate both SISL and daily sleep. SISL was increased by general or neuronal expression, but not glial expression of RelA (Figure 8D), and was decreased by general or neuronal overexpression, but not glial overexpression of Mesh1 (Figure 9A and 9C), indicating that neuronal, but not glial, ppGpp regulates SISL. RelA (Figure 8E) and Mesh1 (Figure 9B) expression in PI neurons labeled by *Dilp2-Gal4* or R19G10 *Gal4* lines resulted in a change in SISL. By contrast, Dh44-expressing neurons were not involved in ppGpp regulation of SISL because neither RelA expression nor Mesh1 overexpression in Dh44 neurons affected SISL (Figures 8E, 9B, and 9D).

Thus, the Dilp2 neurons that are required for ppGpp regulation of sleep latency and awakening are also involved in its regulation of SISL.

DISCUSSION

We have carried out a genetic screen of P element insertion lines which led to the discovery of a new mutation in the *Drosophila* ppGpp hydrolase Mesh1. Our chemical analysis revealed the presence of ppGpp in *Drosophila*. Our chemo connectomic screen suggests involvement of PI neurons in ppGpp function. Further genetic intersection experiments confirm that ppGpp in specific PI neurons regulates sleep. Our findings indicate that ppGpp is present and has physiological functions in animals. It regulates sleep, including sleep latency and starvation-induced sleep loss.

Evidence for ppGpp Function in *Drosophila*

We obtained evidence for ppGpp function from four series of experiments. First, three mutations in mesh1 caused sleep phenotypes in Drosophila. The first mutation is a P-element

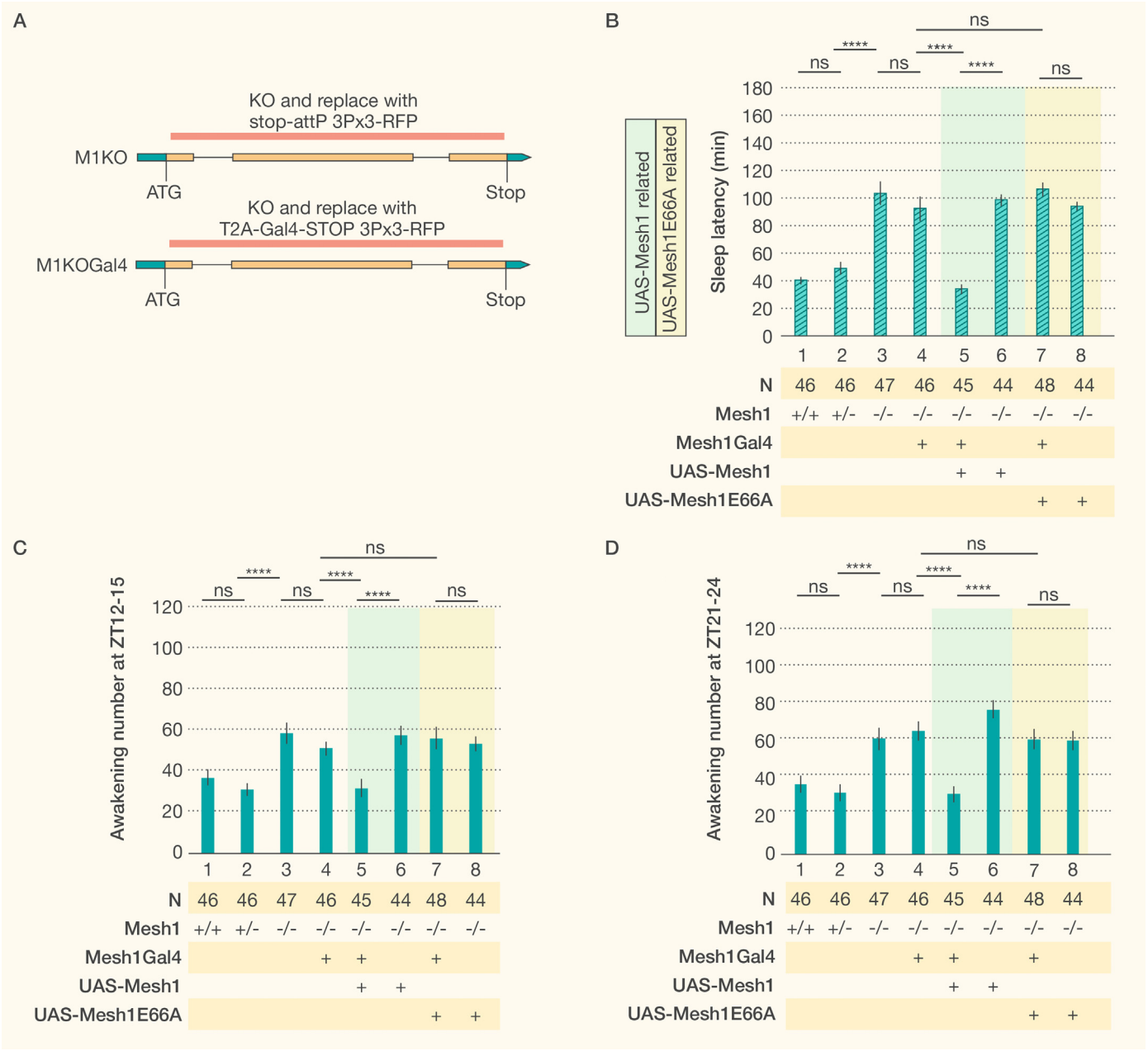

Figure 4. Significance of the hydrolysis activity of Mesh1 in sleep
(A) Schematic representations of *mesh1* gene with the red bar indicating the region deleted in *M1KO* and *M1KOGal4* flies respectively. *mesh1* CDS except the start codon was deleted in both *M1KO* and *M1KOGal4*, and the only difference is that a T2A-fused Gal4 (with a stop codon) was placed in *M1KOGal4*. Sleep latency at night (B), awakening number at early night (C), and awakening number at late night (D) were rescued to wildtype level by expression of Mesh1, but not Mesh1E66A. Numbers of flies used were denoted below each bar. Genotypes from left to right: 1, wildtype; 2, *M1KO/+*; 3, *M1KO/M1KO*; 4, *M1KOGal4/M1KOGal4*; 5, *M1KOGal4/M1KO*, *UAS-Mesh1*; 6, *M1KO/M1KO*, *UASMesh1*; 7, *M1KOGal4/M1KO*, *UAS-Mesh1E66A*; 8, *M1KO/M1KO*, *UAS-Mesh1E66A*. One-way ANOVA and Bonferroni post-tests was used, ***$P < 0.001$, ****$P < 0.0001$. Error bars represent SEM. The number of flies used in the experiment was denoted under each bar.

insertion [53], whose phenotype (Figure 1A and 1B) and molecular nature we have characterized as *mesh1-ins* (Figure 1C). The second mutation is a knockout generated by us as *M1KO* (Figure 1C). The third mutation is a knock-in generated by us as M1KOGal4 (Figure 4A). All three lines have same phenotypes.

Second, we have shown that the hydrolyzing activity of Mesh1 is required to rescue the *mesh1* knockout mutant phenotype: if a point mutation was introduced to amino acid residue 66 by converting it from E to A, then it was enzymatically inactive *in vitro* (Figure S1A) and unable to rescue the sleep and SISL phenotypes *in vivo* (Figures 4 and 8C).

Third, in addition to its role in ppGpp hydrolysis, Mesh1 is recognized as an NADPH phosphatase in mammalian cells [61], and NADH/NADPH ratio has been reported to regulate sleep [74,75]. To determine whether the sleep phenotypes observed in mesh1 mutants are indeed attributed to ppGpp, we showed that 1) disruption of the ppGpp hydrolase activity

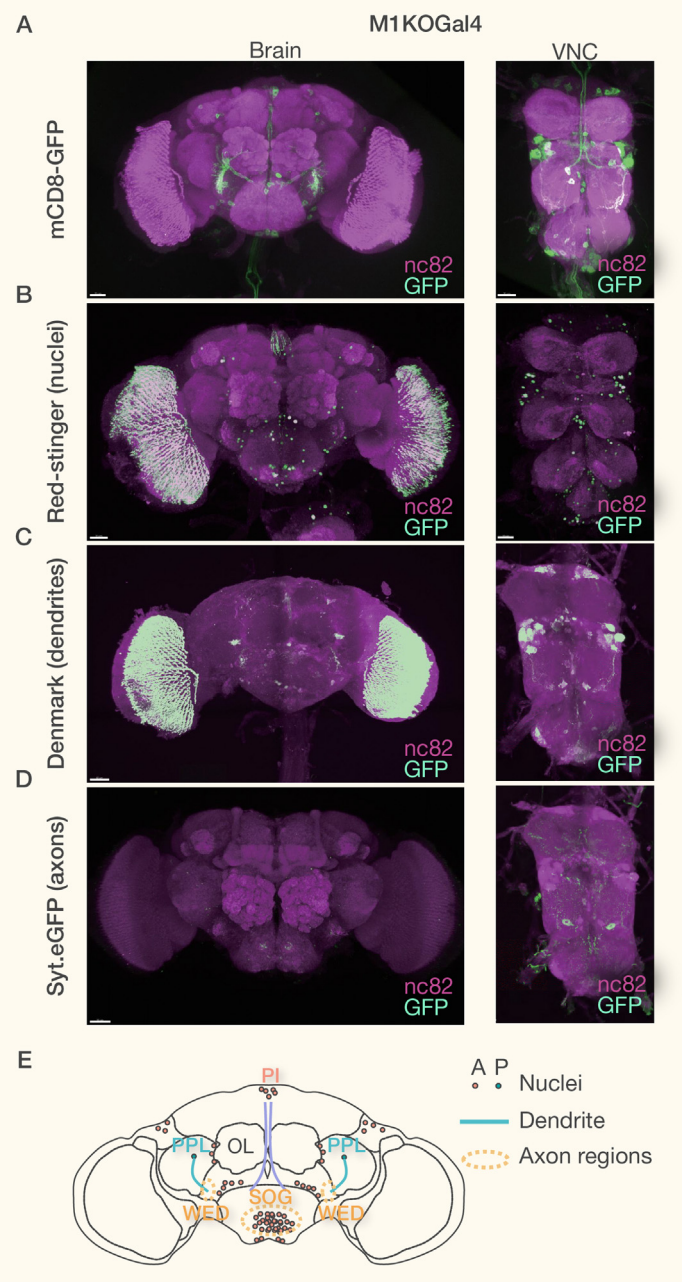

Figure 5. Expression patterns of *mesh1*
Expression patterns of *M1KOGal4* labeled by mCD8-GFP (A), red-stinger (B), Denmark (C), and Syt-eGFP (D) in the brain (left) and the VNC (right), immunostained with anti-GFP (green) and nc82 (magenta). (E) A diagrammatic summary of neurons labeled by *M1KOGal4*. Abbreviations: A, anterior; P, posterior.

in Mesh1E66A expression failed to rescue the sleep phenotype of mesh1 knockout mutants (Figure 4); 2) the ectopic expression of RelA, a bacterial ppGpp synthetase, in Drosophila phenocopied mesh1 knockout mutants (Figures 6 and 8).

Fourth, the phenotypes of Mesh1 overexpression are opposite to those of RelA expression (Figures 7 and 9).

Sleep Regulation Role of ppGpp in Dilp2 Neurons

Does ppGpp function in all cells or only in some cells? Results obtained here support that ppGpp functions in specific neurons in the PI to regulate sleep.

mesh1 gene is expressed in specific neurons (Figure 5). Because Mesh1 is a ppGpp hydrolase, its expression can show the location where ppGpp is hydrolyzed, but not necessarily where it is synthesized or where it functions. When we screened Gal4 lines from CCT to drive the expression of RelA, sleep phenotypes were observed in 6 lines which were all expressed in the PI (Figure S3). When Gal4 lines for PI neurons were used to drive RelA or Mesh1 expression, *Dilp2-Gal4* could indeed cause sleep and SISL phenotypes, while *DH44-Gal4* could not (Figures 6–9). Expression of RelA or Mesh1 in glial cells did not affect sleep.

Because it is difficult to imagine that both synthetase and hydrolase could cause the same multiple phenotypes in the same neurons if these neurons are not where ppGpp functions, our results are most consistent with the idea that ppGpp functions in Dilp2 neurons to regulate sleep and SISL.

ppGpp Synthesis in *Drosophila*

While we have shown that ppGpp is present in *Drosophila* and that it is hydrolyzed by Mesh1 which is expressed in specific neurons, we do not know how ppGpp is synthesized.

RSHs with the synthetase domain exist in both bacteria [14] and plants [26], but not in animals [28,43]. Either animals have evolved another enzyme to synthesize ppGpp, or that ppGpp in *Drosophila* is synthesized by bacteria and transported by specific mechanisms to neurons in the brain.

Plant RSHs are thought to result from lateral gene transfer events from bacteria [3,76]. Bioinformatic analyses and biochemical assays indicate that ppGpp synthetase homologs are distributed widely in plants including dicotyledon *Arabidopsis thalaniana* [26], monocotyledon *Oryza sativa* [27], green algae *Chlamydomonas reinhardtii* [77], *Spiraea japonica* [42], *Nicotiana Tabacum* [34], pea plants [78], *Capsicum annum* [35], and moss *Physcomitrium patens* [38]. Presence of the N-terminal chloroplast transit peptide (cTP), causes most plant RSHs to be located in the chloroplasts [21,24,78–81]. It is unclear whether a ppGpp synthetase exists in *Drosophila* mitochondria.

Molecular Targets of ppGpp

Previous studies have suggested a role of Dilp2 and Dilp2 neurons in sleep regulation under fed and starved conditions [60,73,82]. How does ppGpp function in these neurons to regulate sleep and SISL? In bacteria, the best-known direct target of ppGpp is RNA polymerase (RNAP) [83–87]. ppGpp interaction with the RNA polymerase leads to blockage of transcription initiation [83] and elongation [86]. There are also other possible targets for ppGpp [2,4,88–94].

Similar to its role in the bacterial "stringent response," ppGpp in flies is intricately linked with metabolic status: ppGpp level is increased upon starvation (Figure 2D–2G), and starvation-induced sleep loss is exacerbated in mesh1 mutant flies. While previous studies have established the essential role of Dilp2 (Drosophila insulin-like peptide 2) in starvation-induced sleep loss [73], manipulation of RelA and Mesh1 in Dilp2 neurons affects both sleep and SISL. These findings strongly indicate that ppGpp connects metabolism and sleep regulation.

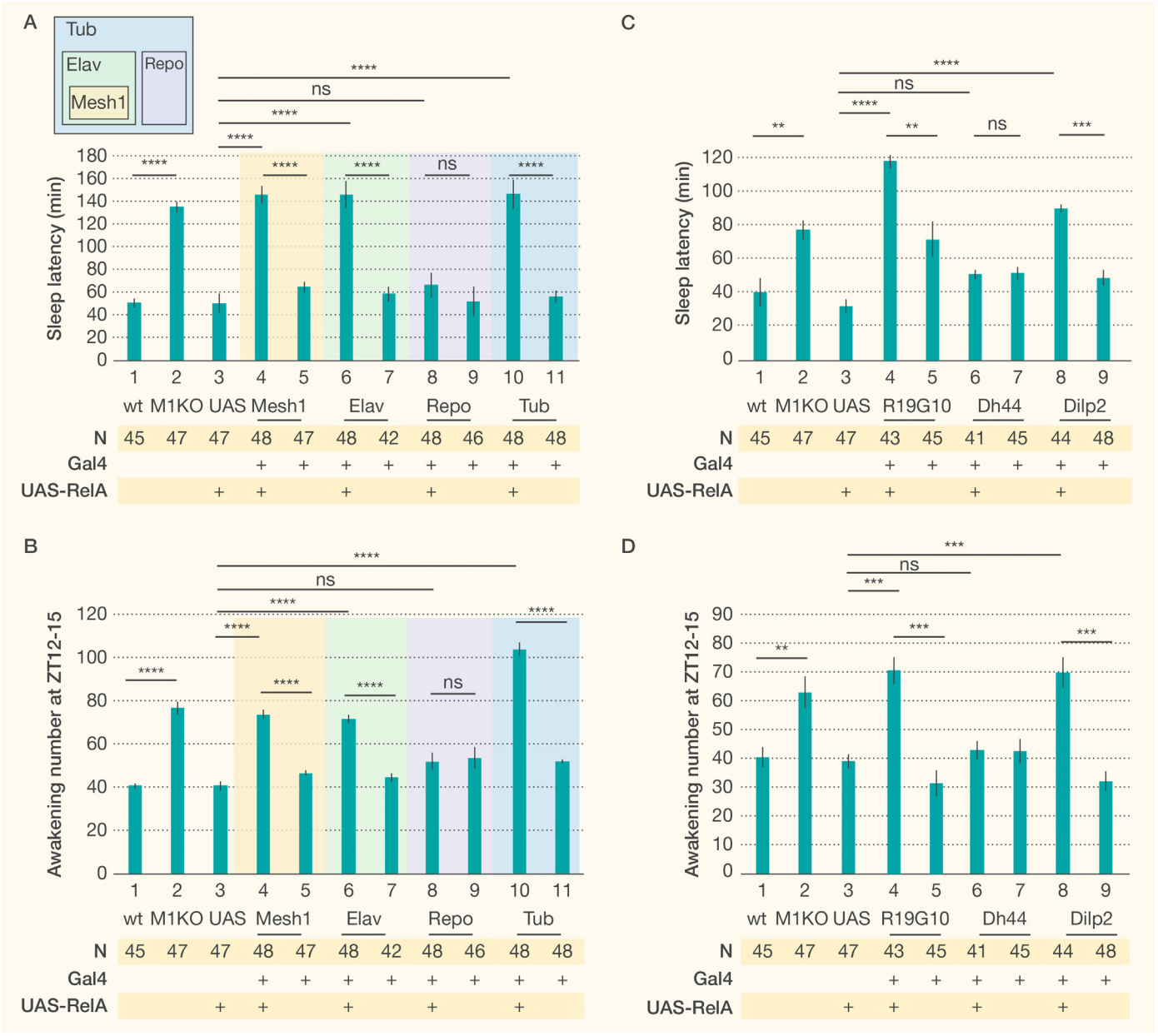

Figure 6. RelA ectopic expression in Dilp2 neurons phenocopies *mesh1* mutants in sleep
Statistical analyses of sleep latency (A) and awakening numbers at early night (B) when RelA was expressed in all cells labeled by *tub-Gal4*, in neurons labeled by *elav-Gal4*, in glia labeled by *repo-Gal4*, or in *mesh1*-expressing cells labeled by *M1KOGal4*. Genotypes from left to right: 1, wildtype; 2, *M1KO/M1KO*; 3, *UAS-RelA/+*; 4, *M1KOGal4/UAS-RelA*; 5, *M1KOGal4/+*; 6, *elav-Gal4/Y;;UAS-RelA/+*; 7, *elav-Gal4/Y*; 8, *repo-Gal4/UAS-RelA*; 9, *repo-Gal4/+*; 10, *tub-Gal4/UAS-RelA*; 11, *tub-Gal4/+*. Statistical analyses of sleep latency (C) and awakening numbers at early night (D) with RelA expression in different subsets of *pars intercerebralis* (PI) neurons. Genotypes from left to right: 1, wildtype; 2, *M1KO/M1KO*; 3, *UAS-RelA/+*; 4, *R19G10-Gal4/UAS-RelA*; 5, *R19G10-Gal4/+*; 6, *Dh44-Gal4/UAS-RelA*; 7, *Dh44-Gal4/+*; 8, *Dilp2-Gal4/+; UAS-RelA/+*; 9, *Dilp2-Gal4/+*. Two-way ANOVA and Bonferroni post-tests was used, $^{**}P < 0.01$, $^{***}P < 0.001$, $^{****}P < 0.0001$. Error bars represent SEM. The number of flies used in the experiment was denoted under each bar.

Moreover, there is compelling molecular evidence supporting the involvement of ppGpp in metabolism: A recent study utilizing a ppGpp-coupled bait uncovered new ppGpp target proteins in bacteria, including a large group of GTPase and metabolism-related enzymes [95]. Metabolome analysis has identified changes in a number of metabolites in Mesh1 Loss of Function (LOF) and Gain of Function (GOF) larvae [22].

Future studies are required to understand the mechanisms and identify the molecule(s) directly mediating sleep and SISL regulation of ppGpp in Dilp2 neurons in *Drosophila*.

MATERIALS AND METHODS

Fly Stocks and Rearing Conditions

All flies were reared on standard corn meal at 25 °C and 60% humidity, under 12 h:12 h LD cycle unless specified otherwise.

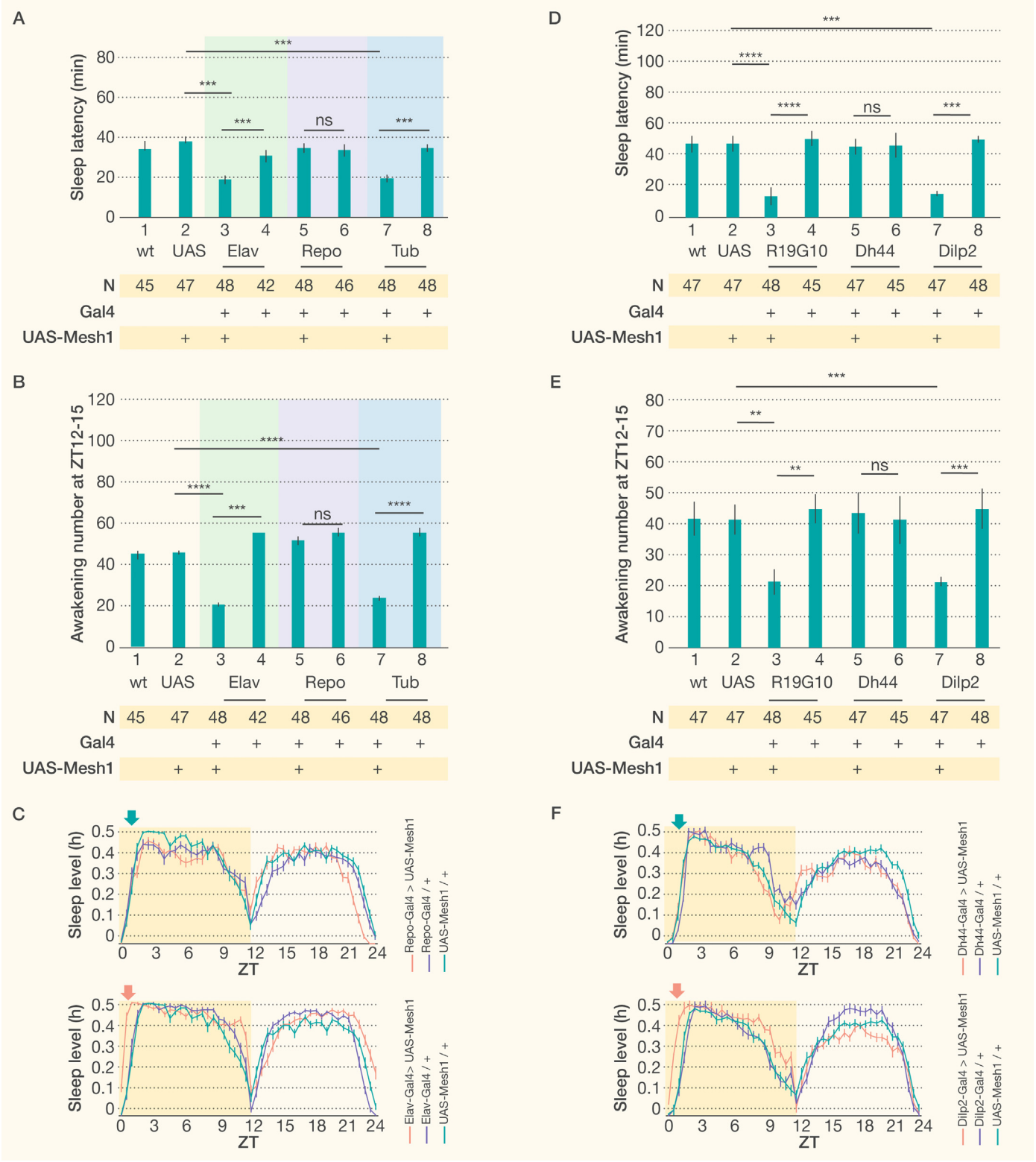

Figure 7. Mesh1 overexpression in subsets of neurons affected sleep

Statistical analyses of sleep latency (A) and awakening numbers at early night (B) when Mesh1 was overexpressed in all cells, neurons, or glia. Genotypes from left to right: 1, wildtype; 2, *UAS-Mesh1*/+; 3, *elav-Gal4/Y;;UAS-Mesh1*/+; 4, *elav-Gal4/Y*; 5, *repo-Gal4/UAS-Mesh1*; 6, *repo-Gal4*/+; 7, *tub-Gal4/UAS-Mesh1*; 8, *tub-Gal4*/+. (C) Representative sleep profiles of lines in (A) and (B) in 30mins bins. Arrows denote sleep latency at early night. *UAS-Mesh1*/+ in the top and bottom panels was the shared control, with the top panel showing that *repo-Gal4>UAS-Mesh1* did not affect sleep latency whereas the bottom panel showing that *elav-Gal4>UAS-Mesh1* shortened sleep latency. (D–E) Statistical analyses of sleep latency (D) and awakening numbers at early night (E) with Mesh1 overexpression in different subsets of PI neurons. Genotypes from left to right: 1, wildtype; 2, *UAS-Mesh1*/+; 3, *R19G10-Gal4/UAS-Mesh1*; 4, *R19G10-Gal4*/+; 5, *Dh44-Gal4/UAS-Mesh1*; 6, *Dh44-Gal4*/+; 7, *Dilp2-Gal4/+; UAS-Mesh1*/+; 8, *Dilp2-Gal4*/+. (F) Representative sleep profiles of lines in (D) and (E). Arrows denote sleep latency at

(legend continued on next page)

Before behavioral assays, stocks were backcrossed into the background of an isogenized Canton S wt line in the lab for 7 generations.

Lines ordered from the Bloomington Stock Center included: #458 (elav-Gal4), #7415 (repo-Gal4), #47887 (R19G10-Gal4), #51987 (Dh44-Gal4), nos-phiC31, #37516 (Dilp2-Gal4), #5137 (UAS-mCD8-GFP). P-element insertion collection was a gift from Dr. U Heberlein (Janelia Research Campus) [96], and CCT-Gal4 library was a collection previously generated in our lab [65]. isoCS and w^{1118} were wild-type and white-eye wild-type lines.

Reagents and Plasmids

PCR was performed with Phanta-Max Super-Fidelity DNA Polymerase (Vazyme, Nanjing, JiangSu, China). Genotyping PCR was performed with 2x Taq PCR StarMix with Loading Dye (GenStar, Shanghai, China). Restriction enzymes *Kpn*I-HF, *Sac*II, *Not*I-HF, *Xba*I, *Xho*I, *BamH*I-HF, *Dpn*I, *EcoR*I-HF, and *Xba*I were from New England BioLabs. Total RNA was extracted from flies with RNAprep pure Tissue Kit (TIANGEN, Beijing, China). Reverse transcription for cDNA cloning was performed with PrimeScript™ II 1st Strand cDNA Synthesis kit (Takara, Shiga, Japan), and Gibson assembly was performed with NEBuilder HiFi DNA Assembly Master Mix (New England Biolabs, Ipswich, MA, USA). Transformation for cloning was performed with Trans-5α (TransGen, Beijing, China), and transformation for expression was performed with Transetta (TransGen, Beijing, China). BL21 (TransGen, Beijing, China) was used as the bacterial gene template. Reverse transcription for quantitative PCR (qPCR) analyses was performed with PrimeScript RT Master Mix kit (Takara, Shiga, Japan). qPCR was performed with TransStart Top Green qPCR SuperMix kit (TransGen, Beijing, China).

pACU2 was a gift from Drs. Lily and Y.N. Jan. The plasmids previously used in our lab included: pBSK, and pET28a+. Templates of STOP-attP-3Px3-RFP, T2A-Gal4-3Px3-RFP, and T2A-flp-3Px3-RFP were previously generated in the lab [65].

Molecular Cloning and Generation of Transgenic Flies

Generation of all KO and KI lines was based on the CRISPR-Cas9 system with homologous recombination, according to previous procedures described [97]. U6b vector was used for the transcription of single guide RNA (sgRNA) [97] and construction of targeting vectors was based on previous procedures in our lab [65].

To generate knock-out lines, a mixture of two *in vitro* transcribed U6b-sgRNA and one targeting vector was injected into *Drosophila* embryos. To generate U6b-sgRNA, two sgRNAs were selected on website (https://www.flyrnai.org/crispr), and designed into a pair of primers (M1KOSgRNA-1F, M1KOSgRNA-1R, M1KOSgRNA-2F, and M1KOSgRNA-2R) without PAM sequence. The other pair of primers (U6b-lacZrv and U6b-primer1) were designed to anneal the backbone of U6b vector so that they could generate PCR products containing two parts of U6b (shorter fragment by M1KO sgRNA-F and U6b-lacZrv, longer fragment by M1KO sgRNA-R and U6b-primer1), which share overlapping sequences in both ends. U6b-sgRNA plasmid was built by Gibson-assembly of the PCR products. To generate the targeting vector, two fragments (2kbps) flanking the entire CDS of gene Mesh1 except start codon were cloned as 5′Arm (amplified with genomic DNA with primers M1KO5F and M1KO5R) and 3′ arm (amplified from genomic DNA with primers M1KO3F and M1KO3R). Vector pBSK was digested with *Kpn*I and *Sac*II, and the PCR products were introduced into the digested pBSK by Gibson-assembly. New restriction sites (*Not*I and *Xho*I) were introduced between the two arms for further use. To generate the targeting vector for *M1KO*, STOP-attP-3Px3-RFP was amplified with primers attP2M1KOF and attP2M1KOR, and inserted between *Not*I and *Xho*I by Gibson-assembly; and for *M1KOGal4*, T2A-Gal4-3Px3-RFP was inserted at same location. A mixture of U6b-sgRNAs and the targeting vector was injected into embryos of *nano*-Cas9 or *vasa*-Cas9 [97]. F1 individuals of RFP + eyes were collected after being crossed with w^{1118} flies.

To generate knock-in line *M1KIflp*, similar procedures were performed. For U6b-sgRNA, primers for shorter fragments were M1KISgRNA-1F or M1KISgRNA-2F paired with U6b-lacZrv, while primers for longer fragments were M1KIsgRNA-1R or M1KIsgRNA-2R with U6b-primer1. For the targeting vector, 5′Arm was amplified with M1KI5F and M1KI5R, and 3′Arm with M1KI3F and M1KI3R. The site flanked by two arms was selected near the very end of Mesh1 CDS so that the stop codon was removed and the CDS was fused with T2A-flp-3Px3-RFP with primers flp2M1KIF and flp2M1KIR.

Generation of transgenic UAS lines was based on vector pACU2 [98]. *Drosophila* cDNA was generated by reverse transcription from total RNA. By using the cDNA as a template, Mesh1 CDS was amplified with primers (M1CDSF and M1CDSR), and inserted into digested pBSK (by *EcoR*I and *Kpn*I). Point mutation of Mesh1E66A was generated from this plasmid with primers M1E66AF and M1E66AR. Both Mesh1 CDS and Mesh1E66A were cloned with primers M1ACU2F and M1ACU2R. RelA sequence was cloned from BL21 bacteria with primers RAACU2F and RAACU2R. All the above were inserted into digested pACU2 (*Eco*RI with *Xba*I) by Gibson assembly. pACU2 constructs were inserted into attP2 by nos-phiC31 during embryo injection.

The sequence of primers is listed in Table S1.

Molecular Cloning and Inducible Expression in Bacteria

pET28a+ was used for bacterial expression of Mesh1 and RelA proteins. Mesh1 CDS and Mesh1E66A were generated with primers M1ET28F and M1ET28R. RelA was cloned from BL21 bacteria with primers RAET28F and RAET28R. They were inserted into pET28a + by Gibson assembly. Competent cells

early night. Note that the *UAS-Mesh1/+* profile in the top and bottom panels was the shared control, with the top panel showing that *Dh44-Gal4>UAS-Mesh1* did not affect sleep latency whereas the bottom panel showing that *Dilp2-Gal4>UAS-Mesh1* shortened sleep latency. Two-way ANOVA and Bonferroni post-tests was used, $^{**}P < 0.01$, $^{***}P < 0.001$, $^{****}P < 0.0001$. Error bars represent SEM. The number of flies used in the experiment was denoted under each bar.

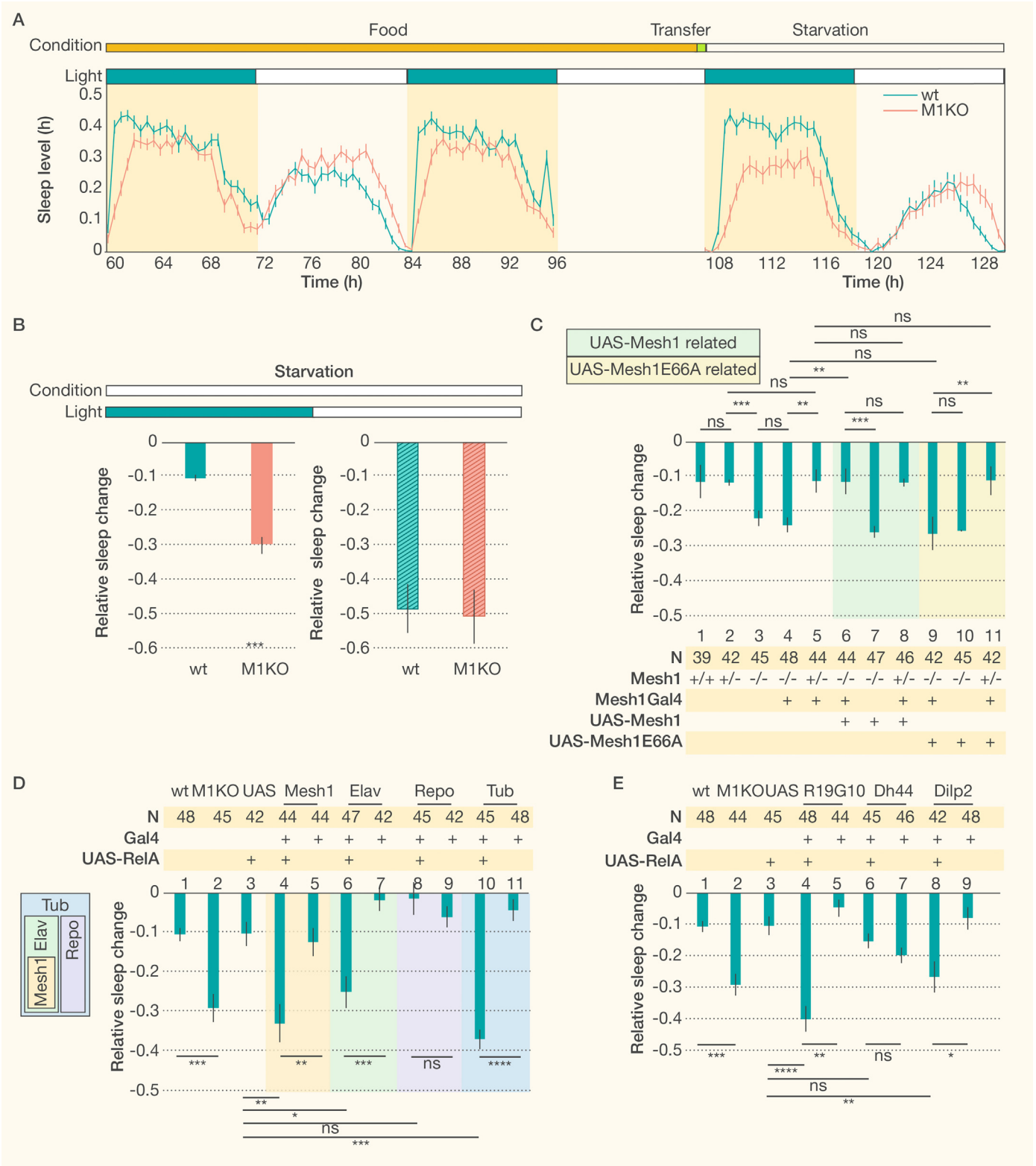

Figure 8. *mesh1* mutants and RelA ectopic expression in Dilp2 neurons both exacerbated SISL

(A) Sleep profiles of wt and *M1KO* flies before and after starvation. Flies were entrained for 3 days (recording at day 2 and day 3), transferred to 1% agar at the end of the 3rd day, followed by sleep recording with starvation of 24h. (B) Statistical analysis of SISL in (A). Sleep loss was significantly exacerbated in *M1KO* flies at nighttime. (C) Statistical analyses of SISL with Mesh1 and Mesh1E66A rescue experiments. Genotypes from left to right: 1, wildtype; 2, *M1KO/+*; 3, *M1KO/M1KO*; 4, *M1KOGal4/M1KO*; 5, *M1KOGal4/+*; 6, *M1KOGal4/M1KO, UAS-Mesh1*; 7, *M1KO/M1KO, UAS-Mesh1*; 8, *M1KOGal4/UAS-Mesh1*; 9, *M1KOGal4/M1KO, UAS-Mesh1E66A*; 10, *M1KO/M1KO, UAS-Mesh1E66A*; 11, *M1KOGal4/UAS-Mesh1E66A*. (D) Statistical analyses of SISL with RelA expression in all cells, neurons, glia or *mesh1*-expressing cells. Genotypes from left to right: 1, wildtype; 2, *M1KO/M1KO*; 3, *UAS-RelA/+*; 4, *M1KOGal4/UAS-RelA*; 5, *M1KOGal4/+*; 6, *elav-Gal4/Y;;UAS-RelA/+*; 7, *elav-Gal4/Y*; 8, *repo-Gal4/UAS-RelA*; 9, *repo-Gal4/+*; 10, *tub-Gal4/UAS-RelA*; 11, *tub-Gal4/+*. (E) Statistical analyses of SISL with RelA

(legend continued on next page)

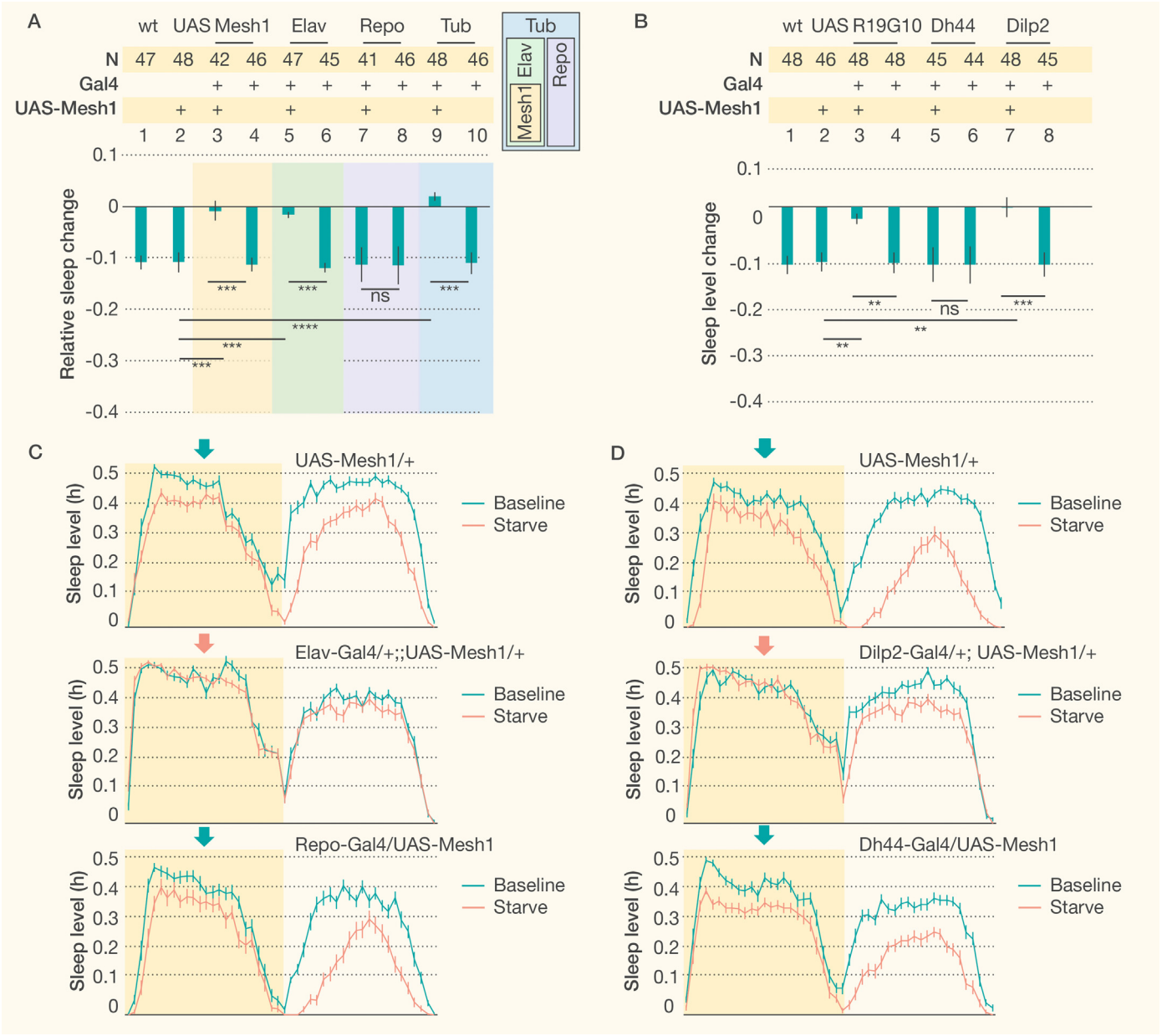

Figure 9. Mesh1 overexpression in Dilp2 neurons reduced SISL
(A) Statistical analyses of SISL with Mesh1 overexpression in neurons or other cells. Genotypes from left to right: 1, wildtype; 2, *UAS-Mesh1/+*; 3, *M1KOGal4/UAS-Mesh1*; 4, *M1KOGal4/+*; 5, *elav-Gal4/Y;;UAS-Mesh1/+*; 6, *elav-Gal4/Y*; 7, *repo-Gal4/UAS-Mesh1*; 8, *repo-Gal4/+*; 9, *tub-Gal4/UAS-Mesh1*; 10, *tub-Gal4/+*. (B) Statistical analyses of SISL with Mesh1 overexpression in different subsets of PI neurons. Genotypes from left to right: 1, wildtype; 2, *UAS-Mesh1/+*; 3, *R19G10-Gal4/UAS-Mesh1*; 4, *R19G10-Gal4/+*; 5, *Dh44-Gal4/UAS- Mesh1*; 6, *Dh44-Gal4/+*; 7, *Dilp2-Gal4/+; UAS- Mesh1/+*; 8, *Dilp2-Gal4/+*. (C) Representative sleep profiles of SISL in (A). Baseline sleep is in green, and sleep during starvation is in orange. Green arrows indicate that night SISL is comparable with wt; Orange arrows indicate night SISL was diminished. (D) Representative sleep profiles of SISL in (B). Two-way ANOVA and Bonferroni post-tests was used, $^{**}P < 0.01$, $^{***}P < 0.001$, $^{****}P < 0.0001$. Error bars represent SEM. The number of flies used in the experiment was denoted above each bar.

were transformed with the above constructs, and the strains were grown for inducible expression. To induce expression, a colony was inoculated into 1 mL kanamycin-containing Luria broth (LB) medium, and incubated at 37 °C for 2 h. 800 μL was transferred into a flask with 800 mL kanamycin + LB media and incubated for ~3 h at 37 °C 220 rpm, until OD_{600} was 0.5–0.6.800 μL 1M isopropyl β-D-1 thiogalactopyranoside (IPTG) was added into the flask. For RelA, the induction was at 37 °C

ectopic expression in different subsets of PI neurons. Genotypes from left to right: 1, wildtype; 2, *M1KO/M1KO*; 3, *UAS- RelA/+*; 4, *R19G10-Gal4/UAS-RelA*; 5, *R19G10-Gal4/+*; 6, *Dh44-Gal4/UAS-RelA*; 7, *Dh44-Gal4/+*; 8, *Dilp2-Gal4/+; UAS-RelA/+*; 9, *Dilp2-Gal4/+*. Student's t-test was used in (B), two-way ANOVA and Bonferroni post-tests was used in (C)–(E), $^{**}P < 0.01$, $^{***}P < 0.001$, $^{****}P < 0.0001$. Error bars represent SEM. The number of flies used in the experiment was denoted under each bar.

for 3 h; for Mesh1 and Mesh1E66A, it was at 16 °C for 16 h. Bacteria was harvested by centrifugation followed by lysis with ultrasonication (Power: 30%, lysis 2 s, wait 2 s, 30 cycles) and centrifugation. Supernatants were passed through nickel columns, followed by two times of wash with 10 mL binding buffer (20 mM Tris–HCl pH 7.4, 0.5 M NaCl, 5 mM imidazole), and eluted with 5 mL elution buffer (20 mM Tris–HCl pH 7.4, 0.5 M NaCl, 500 mM imidazole). Each step was monitored on 10% SDS-PAGE to check protein expression. Eluted protein was enriched in Millipore Amicon Ultra-15, and resuspended in 1 mL of protein storage buffer (20 mM Tris–HCl pH 7.4, 150 mM NaCl, 0.3% CHAPS, 1 mM DTT).

Generation of Germ-Free Flies

Replace the sponge of bottle containing standard fly medium with autoclavable PP bag, and autoclave twice. Evaporate water from food surface in laminar hood and under UV light for 1 h.

According to previous report [99], prepare a simple device for Drosophila egg collection and filter for egg wash, and use the device to collect fly eggs for 5 h, while filters were soaked in 75% EtOH overnight.

Prepare 5 x 50 mL centrifuge tubes, filled with the following solutions: A. 3.3% Walsh hand sanitizer; B. 75% EtOH; C. 1% active chlorine; D. 0.1% TritonX-100 + phosphate-buffered saline (PBS) (1x); E. sterilized ddH_2O.

Use cell scraper to collect eggs onto filters, wash filters from A to E, and disperse the resuspended eggs onto autoclaved fly medium.

Keep rearing at clean incubator for 20 days, and amplify the generated germ-free flies.

Extraction and Measurement of ppGpp

To extract ppGpp from Drosophila, 3 mL formic acid was added to every 250 flies. After grinding for 15 s, 1 mL 30% tri-chloric acetic acid was added to precipitate proteins. The above procedures were repeated to collect extracts from 2000 flies. Supernatants were lyophilized overnight, and powders were resuspended with 200 μL water.

To measure the level of ppGpp, C18 column was used in UPLC-MS, according to a modified version of previous method [100]. The mobile phase included: Buffer A (8 mM N,*N*-dimethylhexylamine, 160 μL acetic acid, 500 mL water) and Buffer B (Acetonitrile). The UPLC program was: at 0min, A:B = 100%: 0; at 10 min, A:B = 40%: 60%, with linear increment. The *m/z* of ppGpp should be 601.95, and ATP (506.00) was used for normalization.

Behavioral Assays

To analyze baseline sleep under 12 h:12 h L:D cycles, approximately 48 flies of each genotype were loaded into glass tubes for video tracing (fps = 1), which was analyzed by an in-house software as described previously [51,65,101]. Continuous immobility of >5min was defined as a sleep bout [45,46]. Sleep latency at early night was defined as the time from light-off (ZT12) to the point when the 1st sleep bout appeared.

To analyze awakening numbers, video-traced data was converted to data of simulated beam-crossing. In the simulation, the middle line for each tube was set as the virtual beam. According to a previous study [55], brief awakening was defined as 1 cross per min, and the awakening number was the sum of such events every 30 min. Awakening number of early night was the sum of brief awakenings at ZT12-15, and awakening number of late night was the sum of brief awakenings at ZT21-24.

To test starvation-induced sleep loss (SISL), sleep was recorded for the first 3 days after flies were loaded into tubes (the 3rd day defined as baseline), and then flies were quickly transferred to tubes of 1 % agar at the end of the light phase of 3rd day, followed by a 24 h recording of sleep during starvation. SISL ratio was defined as (starvation sleep-baseline sleep)/baseline sleep.

Immunohistochemistry and Imaging

To prepare flies for imaging, 5 flies per genotype were dissected in PBS. Dissected tissues were transferred to a tube of 400 μL 2% PFA, and fixed for 55 min. Tissues were washed 3 times with 400 μL brain wash buffer (PBS containing 1% TritonX-100, 3% m/V NaCl), and then transferred to 400 μL blocking buffer (PBS containing 2% TritonX-100, 10% normal goat serum), followed by incubation at 4 °C overnight. Tissues were then transferred to dilution buffer (0.25% TritonX-100, 1% NGS, 1x PBS) and added with primary antibodies. Tissues were stained at 4 °C overnight, followed by 3 washes with 400 μL brain wash buffer. Samples were transferred to fresh dilution buffer containing secondary antibodies (1:200 Alexa Fluor goat anti-chick 488 (Invitrogen, Waltham, MA, USA) and 1:200 Alexa Fluor goat anti-mouse 633 (Invitrogen, Waltham, MA, USA), followed by 3 washes with 400 μL brain wash buffer. Samples were then mounted on slides in Focus Clear (Cell Explorer Labs, FC-101), and imaged on Zeiss LSM 710 confocal microscope (Germany).

Chicken anti-GFP (1:1000) (Abcam Cat# 13970; RRID:AB_300798, Cambridge, UK) and mouse anti-Bruchpilot (1:40) (DSHB Cat# 2314866, nc82; RRID: AB_2314866, Iowa City, IA, USA) were used as primary antibodies with AlexaFluor488 anti-chicken (1:500) (Life Technologies Cat# A11039; RRID:AB_2534096, Carlsbad, CA, USA) and AlexaFluor633 anti-mouse (1:500) (Life Technologies Cat# A21052; RRID: AB_141459, Carlsbad, CA, USA) being used as respective secondary antibodies.

Statistical analyses

Student's *t*-test was used to compare between two groups. One-way ANOVA and Bonferroni post-tests were used to compare multiple groups. All the experiments have been repeated for at least three times with biological replicates.

ACKNOWLEDGMENTS

We are grateful to Dr. U. Heberlein for sharing the P-element insertion mutant library, Drs. J. Ni and G. Gao for providing us with CRISPR/Cas9 plasmids and flies, to Dr. Z.F. Gong for sharing antibodies, to the National Natural Science Foundation of China (32061143017 to Y.R.) and the Research Unit of Medical Neurobiology, Chinese Academy of Medical Sciences (No. 2019RU003) for grant support.

DECLARATION OF COMPETING INTEREST

The authors declare that they have no known competing financial interests or personal relationships that could have appeared to influence the work reported in this article.

ETHICS APPROVAL

Ethics approval is not required for *Drosophila* study.

DATA AVAILABILITY

Further information and requests for resources and reagents should be directed to and will be fulfilled by the Lead Contact, Yi Rao (yrao@pku.edu.cn).

Strains and plasmids are available upon request. The authors affirm that all data necessary for confirming the conclusions of the article are present within the article, figures, and tables.

AUTHOR CONTRIBUTIONS

Y.R. and W.Z. supervised the project. X.D., W.Y., and E.Z. initiated the project and carried out experiments of sleep screen on P-element insertion mutants. W.Y. and T.W. performed the experiments and data analysis. X.Z., Y.L., and X.Z. carried out experiments of UPLC-MS. W.Y. and E.Z. implemented the fly tracing program and developed software for sleep analyses. X.D., W.Y., R.M. and Y.R. wrote and revised the manuscript.

SUPPLEMENTARY DATA

Supplementary data to this article can be found online at https://doi.org/10.1016/j.hlife.2023.10.004.

REFERENCES

[1] Cashel M, Gallant J. Two compounds implicated in the function of the RC gene of *Escherichia coli*. *Nature* 1969;221:838–41.

[2] Dalebroux ZD, Swanson MS. ppGpp: magic beyond RNA polymerase. *Nat Rev Microbiol* 2012;10:203–12.

[3] Field B. Green magic: regulation of the chloroplast stress response by (p)ppGpp in plants and algae. *J Exp Bot* 2018;69:2797–807.

[4] Gourse RL, Chen AY, Gopalkrishnan S, Sanchez-Vazquez P, Myers A, Ross W. Transcriptional responses to ppGpp and DksA. *Annu Rev Microbiol* 2018;72:163–84.

[5] Hauryliuk V, Atkinson GC, Murakami KS, Tenson T, Gerdes K. Recent functional insights into the role of (p)ppGpp in bacterial physiology. *Nat Rev Microbiol* 2015;13:298–309.

[6] Liu K, Bittner AN, Wang JD. Diversity in (p)ppGpp metabolism and effectors. *Curr Opin Microbiol* 2015;24:72–9.

[7] Magnusson LU, Farewell A, Nystrom T. ppGpp: a global regulator in *Escherichia coli*. *Trends Microbiol* 2005;13:236–42.

[8] Potrykus K, Cashel M. ppGpp: still magical? *Annu Rev Microbiol* 2008;62:35–51.

[9] Wang JD, Sanders GM, Grossman AD. Nutritional control of elongation of DNA replication by (p)ppGpp. *Cell* 2007;128:865–75.

[10] Haseltine WA, Block R. Synthesis of guanosine tetra- and pentaphosphate requires the presence of a codon-specific, uncharged transfer ribonucleic acid in the acceptor site of ribosomes. *Proc Natl Acad Sci USA* 1973;70:1564–8.

[11] Hogg T, Mechold U, Malke H, Cashel M, Hilgenfeld R. Conformational antagonism between opposing active sites in a bifunctional RelA/SpoT homolog modulates (p)ppGpp metabolism during the stringent response. *Cell* 2004;117:57–68.

[12] Fangman WL, Neidhardt FC. Protein and ribonucleic acid synthesis in a mutant of *Escherichia coli* with an altered aminoacyl ribonucleic acid synthetase. *J Biol Chem* 1964;239:1844–7.

[13] Yang X, Ishiguro EE. Involvement of the N terminus of ribosomal protein L11 in regulation of the RelA protein of *Escherichia coli*. *J Bacteriol* 2001;183:6532–7.

[14] Cochran JW, Byrne RW. Isolation and properties of a ribosome-bound factor required for ppGpp and ppGpp synthesis in *Escherichia coli*. *J Biol Chem* 1974;249:353–60.

[15] Laffler T, Gallant JA. Stringent control of protein synthesis in *E. coli*. *Cell* 1974;3:47–9.

[16] Leung KL, Yamazaki H. Synthesis of pppGpp by ribosomes from an *Escherichia coli* spoT mutant and the metabolic relationship between pppGpp and ppGpp. *Can J Biochem* 1977;55:1207–12.

[17] Murray KD, Bremer H. Control of spoT-dependent ppGpp synthesis and degradation in *Escherichia coli*. *J Mol Biol* 1996;259:41–57.

[18] Vinella D, Albrecht C, Cashel M, D'Ari R. Iron limitation induces SpoT-dependent accumulation of ppGpp in *Escherichia coli*. *Mol Microbiol* 2005;56:958–70.

[19] Lesley JA, Shapiro L. SpoT regulates DnaA stability and initiation of DNA replication in carbon-starved Caulobacter crescentus. *J Bacteriol* 2008;190:6867–80.

[20] Kessler JR, Cobe BL, Richards GR. Stringent response regulators contribute to recovery from glucose phosphate stress in *Escherichia coli*. *Appl Environ Microbiol* 2017;83.

[21] Boniecka J, Prusinska J, Dabrowska GB, Goc A. Within and beyond the stringent response-RSH and (p)ppGpp in plants. *Planta* 2017;246:817–42.

[22] Ito D, Kato T, Maruta T, Tamoi M, Yoshimura K, Shigeoka S. Enzymatic and molecular characterization of Arabidopsis ppGpp pyrophosphohydrolase, AtNUDX26. *Biosci Biotechnol Biochem* 2012;76:2236–41.

[23] Kasai K, Kanno T, Endo Y, Wakasa K, Tozawa Y. Guanosine tetra- and pentaphosphate synthase activity in chloroplasts of a higher plant: association with 70S ribosomes and inhibition by tetracycline. *Nucleic Acids Res* 2004;32:5732–41.

[24] Sugliani M, Abdelkefi H, Ke H, Bouveret E, Robaglia C, Caffarri S, et al. An ancient bacterial signaling pathway regulates chloroplast function to influence growth and development in *Arabidopsis*. *Plant Cell* 2016;28:661–79.

[25] Tozawa Y, Nozawa A, Kanno T, Narisawa T, Masuda S, Kasai K, et al. Calcium-activated (p)ppGpp synthetase in chloroplasts of land plants. *J Biol Chem* 2007;282:35536–45.

[26] van der Biezen EA, Sun J, Coleman MJ, Bibb MJ, Jones JD. Arabidopsis RelA/SpoT homologs implicate (p)ppGpp in plant signaling. *Proc Natl Acad Sci USA* 2000;97:3747–52.

[27] Xiong L, Lee MW, Qi M, Yang Y. Identification of defense-related rice genes by suppression subtractive hybridization and differential screening. *Mol Plant Microbe Interact* 2001;14:685–92.

[28] Atkinson GC, Tenson T, Hauryliuk V. The RelA/SpoT homolog (RSH) superfamily: distribution and functional evolution of ppGpp synthetases and hydrolases across the tree of life. *PLoS One* 2011;6:e23479.

[29] Irr JD, Kaulenas MS, Unsworth BR. Synthesis of ppGpp by mouse embryonic ribosomes. *Cell* 1974;3:249–53.

[30] Martini O, Irr J, Richter D. Questioning of reported evidence for guanosine tetraphosphate synthesis in a ribosome system from mouse embryos. *Cell* 1977;12:1127–31.

[31] Silverman RH, Atherly AG. Mouse embryos fail to synthesize detectable quantities of guanosine 5'-diphosphate 3'-diphosphate. *Dev Biol* 1977;56:200–5.

[32] Dabrowska G, Prusinska J, Goc A. The stringent response–bacterial mechanism of an adaptive stress response. *Postepy Biochem* 2006;52:87–93.

[33] Fan K, Fisher KM, Edlin G. Effect of amino acid and serum deprivation on the regulation of RNA synthesis in cultured Chinese hamster ovary cells. *Exp Cell Res* 1973;82:111–8.

[34] Givens RM, Lin MH, Taylor DJ, Mechold U, Berry JO, Hernandez VJ, et al. Inducible expression, enzymatic activity, and origin of higher plant homologues of bacterial RelA/SpoT stress proteins in *Nicotiana tabacum*. *J Biol Chem* 2004;279:7495–504.

[35] Kim HM, Ryou SM, Song WS, Sim SH, Cha CJ, Han SJ, et al. Genetic analysis of the invariant residue G791 in *Escherichia coli* 16S rRNA implicates RelA in ribosome function. *J Bacteriol* 2009;191:2042–50.

[36] Mamont P, Hershko A, Kram R, Schacter L, Lust J, Tomkins GM. The pleiotypic response in mammalian cells: search for an intracellular mediator. *Biochem Biophys Res Commun* 1972;48:1378–84.

[37] Rapaport E, Berkley PD, Bucher NL. Charcoal adsorption assay for measurement of colchicine binding and tubulin content of crude tissue extracts. *Anal Biochem* 1975;69:92–9.

[38] Sato M, Takahashi T, Ochi K, Matsuura H, Nabeta K, Takahashi K. Overexpression of RelA/SpoT homologs, PpRSH2a and PpRSH2b, induces the growth suppression of the moss *Physcomitrella patens*. *Biosci Biotechnol Biochem* 2015;79:36–44.

[39] Smulson M. Amino acid deprivation of human cells: effects on RNA synthesis, RNA polymerase, and ribonucleoside phosphorylation. *Biochim Biophys Acta* 1970;199:537–40.

[40] Thammana P, Buerk RR, Gordon J. Absence of ppGpp production in synchronised Balb/C mouse 3T3 cells on isoleucine starvation. *FEBS Lett* 1976;68:187–90.

[41] Thompson LH, Harkins JL, Stanners CP. A mammalian cell mutant with a temperature-sensitive leucyl-transfer RNA synthetase. *Proc Natl Acad Sci USA* 1973;70:3094–8.

[42] Yamada A, Tsutsumi K, Tanimoto S, Ozeki Y. Plant RelA/SpoT homolog confers salt tolerance in *Escherichia coli* and Saccharomyces cerevisiae. *Plant Cell Physiol* 2003;44:3–9.
[43] Sun D, Lee G, Lee JH, Kim HY, Rhee HW, Park SY, et al. A metazoan ortholog of SpoT hydrolyzes ppGpp and functions in starvation responses. *Nat Struct Mol Biol* 2010;17:1188–94.
[44] Ito D, Kawamura H, Oikawa A, Ihara Y, Shibata T, Nakamura N, et al. ppGpp functions as an alarmone in metazoa. *Commun Biol* 2020;3:671.
[45] Hendricks JC, Finn SM, Panckeri KA, Chavkin J, Williams JA, Sehgal A, et al. Rest in *Drosophila* is a sleep-like state. *Neuron* 2000;25:129–38.
[46] Shaw J, Brody S. Circadian rhythms in *Neurospora*: a new measurement, the reset zone. *J Biol Rhythm* 2000;15:225–40.
[47] Artiushin G, Sehgal A. The *Drosophila* circuitry of sleep-wake regulation. *Curr Opin Neurobiol* 2017;44:243–50.
[48] Shafer OT, Keene AC. The regulation of *Drosophila* sleep. *Curr Biol* 2021;31:R38–49.
[49] Danguir J, Nicolaidis S. Dependence of sleep on nutrients' availability. *Physiol Behav* 1979;22:735–40.
[50] Keene AC, Duboue ER, McDonald DM, Dus M, Suh GS, Waddell S, et al. Clock and cycle limit starvation-induced sleep loss in *Drosophila*. *Curr Biol* 2010;20:1209–15.
[51] Dai X, Zhou E, Yang W, Zhang X, Zhang W, Rao Y. D-Serine made by serine racemase in *Drosophila* intestine plays a physiological role in sleep. *Nat Commun* 2019;10:1986.
[52] Dai X, Zhou E, Yang W, Mao R, Zhang W, Rao Y. Molecular resolution of a behavioral paradox: sleep and arousal are regulated by distinct acetylcholine receptors in different neuronal types in *Drosophila*. *Sleep* 2021;44:44.
[53] Eddison M, Belay AT, Sokolowski MB, Heberlein U. A genetic screen for olfactory habituation mutations in *Drosophila*: analysis of novel foraging alleles and an underlying neural circuit. *PLoS One* 2012;7:e51684.
[54] Ronneau S, Hallez R. Make and break the alarmone: regulation of (p)ppGpp synthetase/hydrolase enzymes in bacteria. *FEMS Microbiol Rev* 2019;43:389–400.
[55] Tabuchi M, Monaco JD, Duan G, Bell B, Liu S, Liu Q, et al. Clock-generated temporal codes determine synaptic plasticity to control sleep. *Cell* 2018;175:1213–27.e1218.
[56] Lee T, Luo L. Mosaic analysis with a repressible cell marker for studies of gene function in neuronal morphogenesis. *Neuron* 1999;22:451–61.
[57] Barolo S, Castro B, Posakony JW. New Drosophila transgenic reporters: insulated P-element vectors expressing fast-maturing RFP. *Biotechniques* 2004;36:436–40.
[58] Nicolai LJ, Ramaekers A, Raemaekers T, Drozdzecki A, Mauss AS, Yan J, et al. Genetically encoded dendritic marker sheds light on neuronal connectivity in Drosophila. *Proc Natl Acad Sci USA* 2010;107:20553–8.
[59] Zhang YQ, Rodesch CK, Broadie K. Living synaptic vesicle marker: synaptotagmin-GFP. *Genesis* 2002;34:142–5.
[60] Crocker A, Shahidullah M, Levitan IB, Sehgal A. Identification of a neural circuit that underlies the effects of octopamine on sleep:wake behavior. *Neuron* 2010;65:670–81.
[61] Ding CC, Rose J, Sun T, Wu J, Chen PH, Lin CC, et al. MESH1 is a cytosolic NADPH phosphatase that regulates ferroptosis. *Nat Metab* 2020;2:270–7.
[62] O'Donnell KH, Chen CT, Wensink PC. Insulating DNA directs ubiquitous transcription of the *Drosophila* melanogaster alpha 1-tubulin gene. *Mol Cell Biol* 1994;14:6398–408.
[63] Robinow S, White K. Characterization and spatial distribution of the ELAV protein during *Drosophila* melanogaster development. *J Neurobiol* 1991;22:443–61.
[64] Halter DA, Urban J, Rickert C, Ner SS, Ito K, Travers AA, et al. The homeobox gene repo is required for the differentiation and maintenance of glia function in the embryonic nervous system of *Drosophila* melanogaster. *Development* 1995;121:317–32.
[65] Deng B, Li Q, Liu X, Cao Y, Li B, Qian Y, et al. Chemoconnectomics: mapping chemical transmission in *Drosophila*. *Neuron* 2019;101:876–893.e874.
[66] Cannell E, Dornan AJ, Halberg KA, Terhzaz S, Dow JAT, Davies SA. The corticotropin-releasing factor-like diuretic hormone 44 (DH44) and kinin neuropeptides modulate desiccation and starvation tolerance in *Drosophila melanogaster*. *Peptides* 2016;80:96–107.
[67] Chen YD, Dahanukar A. DH44 neurons: gut-brain amino acid sensors. *Cell Res* 2018;28:1048–9.
[68] Semaniuk UV, Gospodaryov DV, Feden'ko KM, Yurkevych IS, Vaiserman AM, Storey KB, et al. Insulin-like peptides regulate feeding preference and metabolism in *Drosophila*. *Front Physiol* 2018;9:1083.
[69] Yurgel ME, Kakad P, Zandawala M, Nassel DR, Godenschwege TA, Keene AC. A single pair of leucokinin neurons are modulated by feeding state and regulate sleep-metabolism interactions. *PLoS Biol* 2019;17:e2006409.
[70] Collin C, Hauser F, Krogh-Meyer P, Hansen KK, Gonzalez de Valdivia E, Williamson M, et al. Identification of the *Drosophila* and Tribolium receptors for the recently discovered insect RYamide neuropeptides. *Biochem Biophys Res Commun* 2011;412:578–83.
[71] Ohno H, Yoshida M, Sato T, Kato J, Miyazato M, Kojima M, et al. Luqin-like RYamide peptides regulate food-evoked responses in *C. elegans*. *eLife* 2017;6.
[72] MacFadyen UM, Oswald I, Lewis SA. Starvation and human slow-wave sleep. *J Appl Physiol* 1973;35:391–4.
[73] Brown EB, Shah KD, Faville R, Kottler B, Keene AC. *Drosophila* insulin-like peptide 2 mediates dietary regulation of sleep intensity. *PLoS Genet* 2020;16:e1008270.
[74] Kempf A, Song SM, Talbot CB, Miesenbock G. A potassium channel beta-subunit couples mitochondrial electron transport to sleep. *Nature* 2019;568:230–4.
[75] Mariano V, Kanellopoulos AK, Aiello G, Lo AC, Legius E, Achsel T, et al. SREBP modulates the NADP(+)/NADPH cycle to control night sleep in *Drosophila*. *Nat Commun* 2023;14:763.
[76] Ito D, Ihara Y, Nishihara H, Masuda S. Phylogenetic analysis of proteins involved in the stringent response in plant cells. *J Plant Res* 2017;130:625–34.
[77] Kasai K, Usami S, Yamada T, Endo Y, Ochi K, Tozawa Y. A RelA-SpoT homolog (Cr-RSH) identified in Chlamydomonas reinhardtii generates stringent factor *in vivo* and localizes to chloroplasts *in vitro*. *Nucleic Acids Res* 2002;30:4985–92.
[78] Takahashi K, Kasai K, Ochi K. Identification of the bacterial alarmone guanosine 5'-diphosphate 3'-diphosphate (ppGpp) in plants. *Proc Natl Acad Sci USA* 2004;101:4320–4.
[79] Chen J, Bang WY, Lee Y, Kim S, Lee KW, Kim SW, et al. AtObgC-AtRSH1 interaction may play a vital role in stress response signal transduction in *Arabidopsis*. *Plant Physiol Biochem* 2014;74:176–84.
[80] Mizusawa K, Masuda S, Ohta H. Expression profiling of four RelA/SpoT-like proteins, homologues of bacterial stringent factors, in *Arabidopsis thaliana*. *Planta* 2008;228:553–62.
[81] Sato M, Takahashi K, Ochiai Y, Hosaka T, Ochi K, Nabeta K. Bacterial alarmone, guanosine 5'-diphosphate 3'-diphosphate (ppGpp), predominantly binds the beta' subunit of plastid-encoded plastid RNA polymerase in chloroplasts. *Chembiochem* 2009;10:1227–33.
[82] Cong X, Wang H, Liu Z, He C, An C, Zhao Z. Regulation of sleep by insulin-like peptide system in *Drosophila melanogaster*. *Sleep* 2015;38:1075–83.
[83] Artsimovitch I, Patlan V, Sekine S, Vassylyeva MN, Hosaka T, Ochi K, et al. Structural basis for transcription regulation by alarmone ppGpp. *Cell* 2004;117:299–310.
[84] Barker MM, Gaal T, Gourse RL. Mechanism of regulation of transcription initiation by ppGpp. II. Models for positive control based on properties of RNAP mutants and competition for RNAP. *J Mol Biol* 2001;305:689–702.
[85] Kajitani M, Ishihama A. Promoter selectivity of *Escherichia coli* RNA polymerase. Differential stringent control of the multiple promoters from ribosomal RNA and protein operons. *J Biol Chem* 1984;259:1951–7.
[86] Kingston RE, Nierman WC, Chamberlin MJ. A direct effect of guanosine tetraphosphate on pausing of *Escherichia coli* RNA polymerase during RNA chain elongation. *J Biol Chem* 1981;256:2787–97.
[87] Lindahl L, Post L, Nomura M. DNA-dependent *in vitro* synthesis of fibosomal proteins, protein elongation factors, and RNA polymerase subunit alpha: inhibition by ppGpp. *Cell* 1976;9:439–48.
[88] Corrigan RM, Bellows LE, Wood A, Grundling A. ppGpp negatively impacts ribosome assembly affecting growth and antimicrobial tolerance in Gram-positive bacteria. *Proc Natl Acad Sci USA* 2016;113:E1710–9.
[89] Maciag M, Kochanowska M, Lyzen R, Wegrzyn G, Szalewska-Palasz A. ppGpp inhibits the activity of *Escherichia coli* DnaG primase. *Plasmid* 2010;63:61–7.
[90] Nomura Y, Nozawa A, Tozawa Y. Biochemical analyses of ppGpp effect on adenylosuccinate synthetases, key enzymes in purine biosynthesis in rice. *Biosci Biotechnol Biochem* 2014;78:1022–5.
[91] Pao CC, Dyess BT. Effect of unusual guanosine nucleotides on the activities of some *Escherichia coli* cellular enzymes. *Biochim Biophys Acta* 1981;677:358–62.
[92] Paul BJ, Berkmen MB, Gourse RL. DksA potentiates direct activation of amino acid promoters by ppGpp. *Proc Natl Acad Sci USA* 2005;102:7823–8.
[93] Sherlock ME, Sudarsan N, Breaker RR. Riboswitches for the alarmone ppGpp expand the collection of RNA-based signaling systems. *Proc Natl Acad Sci USA* 2018;115:6052–7.
[94] Zhang YE, Baerentsen RL, Fuhrer T, Sauer U, Gerdes K, Brodersen DE. (p)ppGpp regulates a bacterial nucleosidase by an allosteric two-domain switch. *Mol Cell* 2019;74:1239–1249.e1234.
[95] Wang B, Dai P, Ding D, Del Rosario A, Grant RA, Pentelute BL, et al. Affinity-based capture and identification of protein effectors of the growth regulator ppGpp. *Nat Chem Biol* 2019;15:141–50.

[96] Moore MS, DeZazzo J, Luk AY, Tully T, Singh CM, Heberlein U. Ethanol intoxication in *Drosophila*: genetic and pharmacological evidence for regulation by the cAMP signaling pathway. *Cell* 1998;93:997–1007.
[97] Ren X, Sun J, Housden BE, Hu Y, Roesel C, Lin S, et al. Optimized gene editing technology for *Drosophila melanogaster* using germ line-specific Cas9. *Proc Natl Acad Sci USA* 2013;110:19012–7.
[98] Han C, Jan LY, Jan YN. Enhancer-driven membrane markers for analysis of nonautonomous mechanisms reveal neuron-glia interactions in *Drosophila*. *Proc Natl Acad Sci USA* 2011;108:9673–8.
[99] Kietz C, Pollari V, Meinander A. Generating germ-free Drosophila to study gut-microbe interactions: protocol to rear *Drosophila* under axenic conditions. *Curr Protoc Toxicol* 2018;77:e52.
[100] Ihara Y, Ohta H, Masuda S. A highly sensitive quantification method for the accumulation of alarmone ppGpp in *Arabidopsis thaliana* using UPLC-ESI-qMS/MS. *J Plant Res* 2015;128:511–8.
[101] Qian Y, Cao Y, Deng B, Yang G, Li J, Xu R, et al. Sleep homeostasis regulated by 5HT2b receptor in a small subset of neurons in the dorsal fan-shaped body of drosophila. *eLife* 2017;6.